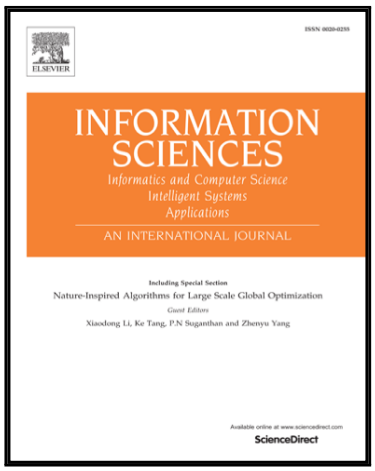

Mobile Data Gathering and Energy Harvesting in Rechargeable Wireless Sensor Networks

Yong Liu, Kam-Yiu Lam, Song Han, Qingchun Chen

PII: S0020-0255(19)30013-1
DOI: https://doi.org/10.1016/j.ins.2019.01.014
Reference: INS 14205

To appear in: *Information Sciences*

Received date: 28 May 2018
Revised date: 9 October 2018
Accepted date: 5 January 2019

Please cite this article as: Yong Liu, Kam-Yiu Lam, Song Han, Qingchun Chen, Mobile Data Gathering and Energy Harvesting in Rechargeable Wireless Sensor Networks, *Information Sciences* (2019), doi: https://doi.org/10.1016/j.ins.2019.01.014

Mobile Data Gathering and Energy Harvesting in Rechargeable Wireless Sensor Networks

Yong Liu[a,b,*], Kam-Yiu Lam[b], Song Han[c], Qingchun Chen[a]

[a] *School of Mechanical and Electrical Engineering, Guangzhou University, Guangzhou, 510006, P.R.China*
[b] *Department of Computer Science, City University of Hong Kong, Kowloon, Hong Kong SAR*
[c] *Department of Computer Science and Engineering, University of Connecticut, Storrs, CT 06269 USA*

Abstract

In this paper, we study the *joint data gathering and energy harvesting* (JoDGE) problem in rechargeable wireless sensor networks (RWSNs) with a mobile sink. In RWSNs, the sensor nodes are equipped with RF circuit to harvest energy from a mobile sink that moves along a pre-defined path, and at the same time, transmit gathered sensor data to the sink. Given that the consumed and harvested energy at a sensor node is proportional and inversely proportional to the square of transmission distance, a *far-relay approach* is proposed to select the sensor nodes closer to the path to assist the data transmission of the farther sensor nodes. Under the *far-relay approach*, we formulate a network utility maximization problem (NUM), and propose an optimal scheduling scheme (Opt-JoDGE), which jointly considers the power allocation, relay selection and time slot scheduling policies. By employing the Lyapunov drift theory, a near optimal buffer-battery-aware adaptive scheduling (NO-BBA) scheme is further proposed, in which the run-time status of the data buffer and battery are utilized. Extensive simulation experiments validate the feasibility and performance of JoDGE and NO-BBA. The results show that the performance of NO-BBA is close to that of Opt-JoDGE, especially when a certain delay is tolerable.

*Corresponding author:Yong Liu
Email addresses: ly454580194@gmail.com (Yong Liu), cskylam@cityu.edu.hk (Kam-Yiu Lam), song.han@uconn.edu (Song Han), qcchen@gzhu.edu.cn (Qingchun Chen)

Keywords: Rechargeable wireless sensor networks (RWSNs), Data gathering, RF energy harvesting, Mobile sink

1. Introduction

One of the challenges in wireless sensor networks (WSNs) is how to gather data from sensors through a resource-constrained wireless network [9]. In WSNs, the sensor nodes periodically sample the physical entities under monitoring, and then transmit the gathered sensor measurements to a sink, which is connected to the rest of the system for data processing and decision making.

In order to improve the sustainability, recently, various energy harvesting technologies have been employed in WSNs [2, 14, 17, 19, 22]. This kind of WSNs is referred to as rechargeable WSNs (RWSNs). Extensive research efforts have been devoted on effective data gathering in RWSNs. For example, [14] proposed an energy-efficient cooperative data collection scheme for clustered RWSNs. In [17], an optimal scheduling algorithm was proposed to minimize data packet loss in RWSNs, where the sink is assumed to be a fixed station.

In RWSNs with static sinks, the transmissions of sensor data to the sinks may pass through one or multiple relay nodes. Thus the sensor nodes geographically closer to the sink usually have to forward more sensor data. Therefore, they are more likely to become the bottleneck of the network due to heavy relay workload. By contrast, data gathering in RWSNs with mobile sink(s) has been shown to be a promising approach to jointly deal with unbalanced traffic distribution and prolong the network lifetime. The mobile sink is assumed to travel along a pre-defined or online-learned path, and the network throughput maximization (NTM) problems were investigated, *e.g.*, through routing and time-slot scheduling [30, 38], joint speed and power control [23], and mobility planning [6, 28, 39, 40]. These works assumed that the sensor nodes harvest energy from either unstable environment sources, *i.e.*, solar and wind, or energy based on magnetic resonance coupling with small charging distance. On the other hand, radio frequency (RF) based energy harvesting seems to be a better

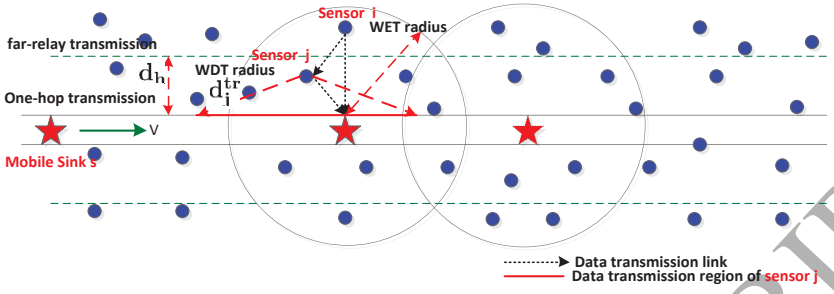

Figure 1: System Model: A rechargeable WSN with one mobile sink on a pre-defined path

potential for RWSNs with mobile sinks, *i.e.*, more stable and controllable with larger effective charging distance.

In this paper, we consider a representative RWSN with a mobile sink using RF based energy harvesting. As shown in Fig. 1, the sink moves along a pre-defined path continuously and repeatedly. While it is moving, nearby sensor nodes harvest energy from the signals emitted by the sink, and at the same time send their sensed data back to the sink. In order to sustain the operations, when gathering data from the sensor nodes, we need to balance the harvested energy and consumed energy at each sensor node. We call this problem as the *joint data gathering and energy harvesting (JoDGE)* problem.

According to the wireless propagation theory [31], the received power level is inversely proportional to the square of transmission distance. Therefore, the nodes that are farther away from the path usually harvest less energy. On the other hand, these nodes may consume more energy for sending data directly to the sink. To reduce the amount of energy consumed in these remote nodes, we propose the *far-relay approach*, in which if a node is far away from the path, it may pass its data to a relay node for forwarding its data to reserve energy, even though it might be able to send the data directly to the sink.

Based on the *far-relay approach*, we formulate the network utility maximization (NUM) problem with energy sustainable constraints to ensure that the energy consumption at each sensor node is always less than its harvested energy, and at the same time the relay selection, power allocation and time slot

scheduling issues are jointly considered. Considering that the primal JoDGE problem is a mixed integer nonlinear problem (MINLP), we reformulate it to be a convex optimization problem through a novel two-step transformation, and derive the optimal Opt-JoDGE scheduling scheme.

To reduce the computation complexity of Opt-JoDGE, we further propose the *near-optimal buffer-battery-aware adaptive data gathering scheduling (NO-BBA)* scheme to solve the JoDGE problem, in which the run-time status of the data buffer and battery of all involved sensor nodes are also exploited.

Finally, we give comprehensive performance analysis for both Opt-JoDGE and NO-BBA. Extensive simulations have also been performed to confirm the feasibility and effectiveness of the proposed schemes and validate our performance analysis. The remainder of this paper is organized as follows: Section 2 presents a literature review on related works. Section 3 introduces the network model. The formulations of the JoDGE problem and Opt-JoDGE scheduling scheme are presented in Section 4. Section 5 introduces the NO-BBA scheme, and the performance results of both Opt-JoDGE and NO-BBA are reported in Section 6. In Section 7, we conclude the paper with a brief discussion on the future work. For the readers' convenience, the symbols and their definitions that are commonly referred in this paper are summarized in Table 1.

2. Related Work

Extending the lifetime of sensors with limited battery energy is a major research challenge in WSNs, and various approaches have been proposed for efficient energy utilization [25, 32, 34, 37]. In [25], a fuzzy logic-based clustering algorithm was presented to extend the network lifetime. In [37], the authors investigated the energy consumption density performance in data gathering, and proposed a directional virtual backbone based data aggregation scheme by employing the directional antennas and virtual backbone techniques.

Energy harvesting (EH) technologies have been introduced to charge the sensor nodes in *rechargeable wireless sensor networks (RWSNs)* to improve

their sustainability. The state-of-the-art of energy harvesting technologies was reviewed for RWSNs in [1]. In RWSNs, energy may be harvested from either surrounding environment [18, 22, 23, 29, 30] or dedicated energy sources [10, 14, 20, 24, 39]. When using dedicated energy sources, wireless charging technologies utilize energy transmitter(s) to charge the sensor nodes wirelessly via either non-radiative coupling or radiative radio-frequency (RF) techniques. As one kind of non-radiative coupling, magnetic resonance coupling is based on evanescent-wave coupling to generate energy between two resonant coils through magnetic field. The most important properties of non-radiative coupling are small charging distance and high efficiency.

RF-based energy harvesting utilize diffused radio-frequency signals as a medium to carry the energy. The energy harvesting model with different transmitter placements was analyzed in [24]. In [10], the authors proposed an energy-efficient software-defined RWSN architecture. [8] studied the optimal scheduling problem for stochastic event capture, i.e., how to jointly mobilize the readers for energy distribution and how to schedule the sensor nodes. [19] exploited the collaborative energy and information transfer to realize the green smart cities via jointly optimize sub-carrier grouping, sub-carrier pairing and power allocation. In [36] the energy-efficiency maximization problem based on the simultaneous wireless information and power transfer (SWIPT) framework was considered, and in [14], the authors incorporated SWIPT into cooperative clustered WSNs, and proposed an efficient cooperative data collection scheme.

Previous studies on WSNs with mobile elements [9] have shown that the mobile sink approach significantly improves the network performance, for instance, balancing the traffic load, reducing transmission delay and enhancing network coverage. However, some new challenges also arise, such as contact detection, power management and so on. Most previous works aimed to maximize network throughput, lifetime under predefined [12] or planned mobility patterns [21, 35].

In [22], a scheme was proposed to jointly control the data buffer and battery in RWSNs to maximize the long-term average throughput under given QoS constraints. The time-slot scheduling approach was presented in [30] for RWSNs

with a mobile sink, in which the sink periodically traveled along a pre-defined path at a constant speed to collect data from sensor nodes within one hop. [38] extended the work of [30] to multi-hop RWSNs, and aimed to maximize the network utility by optimizing power and rate control. The joint power and speed control was studied in [23], where one-hop transmission was assumed and two scenarios with constant and varying speeds were analyzed. A multi-functional mobile entity, called SenCar, was proposed to serve as not only a mobile data collector that roamed over the field to gather data but also an energy source to charge static sensor nodes on its migration tour via wireless energy transmissions. In [28], a greedy scheduling algorithm was proposed to schedule limited mobile devices for energy replenishment and data collection in RWSNs with multiple sinks. In [6], the authors designed a node-Gosper island-based scalable hierarchical cluster transmission method in conjunction with a wireless recharging plan for data collection in RWSNs. In the proposed transmission method, both the magnetic resonance coupling based and RF based energy harvesting technologies were investigated.

Compared to energy harvesting via ambient energy sources and magnetic resonance coupling, RF energy harvesting has a larger effective charging distance, and the amount of harvested energy is inversely proportional to the square of the transmission distance. This indicates that the sensor nodes closer to the path can harvest more energy to support relaying traffic. Meanwhile, RF-energy harvesting is an efficient method to provide reliably guaranteed energy supply [20]. Thus, the energy harvesting via RF radiation is highly suitable for RWSNs. To the best of our knowledge, there is no previous work that jointly considers the sink mobility and RF energy harvesting technology in RWSNs. In our work, the run-time status of the data buffer and battery of each sensor node is also exploited to solve the network utility problem, in which the rate control, power allocation, relay selection and time scheduling problems are jointly considered.

Table 1: Symbols and Definitions

Symbol	Definition
$a_k(t)$	Maximum sensing rate of sensor node k at time slot t
d_0	Reference distance with measured path loss $L_0(d_0)$
d_e	RF energy transfer radius
d_h	Vertical distance threshold of the one-hop manner
d_k^{tr}	Transmission radius of sensor node k
d_{ij}	Distance between node i and node j
$d_{ks}(t)$	Distance between sensor node k and sink at time slot t
$e_k^h(t)$	The amount of energy harvested by sensor node k at slot t
$e_k^c(t)$	The amount of energy consumed by sensor node k at slot t
$\mathbf{e}_k^{sn}$	Energy consumed for sensing data at sensor node k
$e_{ij}(t)$	The energy consumed on the link from nodes i to j
$\|g_{sk}(t)\|^2$	Channel fading gain between sink s and sensor k in WET mode
$\|h_{ij}(t)\|^2$	Channel fading gain between nodes i and j in WDT mode
$r_{ij}(t)$	The amount of bits transmitted from node i to node j at slot t
$\underline{t}_k^e$	Earliest time slot that sensor node k can harvest energy
$\overline{t}_k^e$	Latest time slot that sensor node k can harvest energy
$\underline{t}_k^{tr}$	Earliest slot that sensor node k can transmit data
$\overline{t}_k^{tr}$	Latest time slot that sensor node k can transmit data
$(x_0(t), y_0)$	Position of the sink at time slot t
(x_k, y_k)	Position of sensor node k
$x_k(t)$	Data bits added into the data buffer of sensor node k
α	Path loss exponent
$\tau_{ij}(t)$	Scheduling variable for the link from node i to node j
η	Energy conversion efficiency
$\mathcal{K}$	The set of all sensor nodes
$\mathcal{N}_d$	The set of the sensor nodes in the one-hop manner
$\mathcal{N}_c$	The set of the sensor nodes in the cooperative two-hop manner

continued Table 1

Symbol	Definition
$\mathcal{R}_i$	The set of candidate relay nodes of sensor node i
$L_0(d_0)$	The path loss with reference distance d_0
N	Total number of time slots in one pass
T	Duration of one time slot
P_s	Power of the sink in wireless energy transfer
$P_k(t)$	Power of sensor node k at time slot t
$\mathbf{E}_k(t)$	Battery status of node k at time slot t
$\mathbf{Q}_k(t)$	Data buffer status of sensor node k at time slot t

3. System Model

3.1. Network and Mobility Model

As illustrated in Fig. 1, we consider a rechargeable wireless sensor network (RWSN), in which a mobile sink s moves along a pre-defined path, and a set of K sensor nodes $\mathcal{K} = \{1, 2, 3, \cdots, K\}$ are randomly distributed around the path of the sink. The sensor nodes are organized into a time-slotted network, *e.g.*, based on 802.15.4e MAC protocol [33], and have network-wide synchronization [5]. There are in total N time slots for scheduling data transmissions in one pass (from one end to the other end), and the size of each slot is defined as T.

The sink s moves continuously along a pre-defined path at a constant speed v from one end to the other end (called a *pass*) repeatedly[1]. While s is moving, it receives data from nearby sensor nodes, and also deliveries energy for charging them via radio frequency signal. It is assumed that the sink has enough energy for charging all sensor nodes in the network. As the size of each slot is T, the

[1]Since the sink travels along the path at a constant speed continuously, the length of a periodic cycle from the starting point to the end point or from the end point to the starting point does not affect the performance from a long-term point of view.

distance traveled by the sink in one time slot is equal to $v \cdot T$. It is assumed that T is small enough so that the location of the sink can be assumed to remain unchanged within one time slot. We define (x_0, y_0) as the initial location of the sink at time slot 0. To simplify the discussion, it is assumed that the sink moves along a straight line, *i.e.*, $y_0(t) = y_0$, $x_0(t) \in [0, v \cdot N \cdot T]$. As wireless energy transfer (WET) technology is limited by its effective charging distance, we define d_e as the effective energy transfer radius within which the sensor nodes can harvest energy from the sink successfully. In order to guarantee that all sensor nodes can harvest energy from the sink, we assume that the greatest distance between a sensor node and the path is always less than d_e. In large-scale RWSNs deployment, multiple mobile sinks or a careful trajectory planning may be needed. We defer those studies to our future work.

In order to sustainably sending data, each sensor node is equipped with an RF energy harvesting circuit, and its wireless data transfer (WDT) operation mode and WET operation mode can be performed simultaneously, *e.g.*, by splitting the frequency/time domain or employing separated receiver circuits. In WET mode, a sensor node harvests energy from the RF signals emitted from the sink to charge its own battery; in WDT mode, data collected by a sensor node will be sent to the sink either directly or through other sensor nodes, which act as relay nodes.

We denote (x_k, y_k) as the fixed location of sensor node k, and use d_k^{tr} to represent the transmission range of a sensor node k, within which it can transmit data successfully. Each sensor node has a data buffer to temporarily store the data generated by the sensor node itself or received from other sensor nodes.

3.2. Far-Relay Approach

An important consideration in the JoDGE problem is the *double near-far* problem [15]. In wireless energy transfer, the sensor nodes closer to the path of the sink (the energy source) generally harvest more energy than the sensor nodes which are farther away. On the other hand, the energy consumption is always proportional to the square of the transmission distance. Therefore, the

sensor nodes that are farther away from the path may consume more energy for data transmission but harvest less energy.

Due to the *double near-far* problem, how to maintain sustainable operation of the sensor nodes while improving the network performance, especially how to fulfill the data transmission requirement of the farther sensor nodes, becomes a critical issue. Inspired by wireless powered cooperative communication [7, 14], we propose a *far-relay approach* to address this problem, in which if the physical distance between a sensor node and the path is less than a threshold d_h[2], it will transmit data to the sink directly. Otherwise the sensor node may transmit data in a *selectively cooperative manner* by either choosing a relay node for assisting data transmission or directly transmitting data to the sink.

According to the distance threshold d_h, we divide the sensor nodes into two subsets $\mathcal{N}_c = \{1, 2, \cdots, |\mathcal{N}_c|\}$ and $\mathcal{N}_d = \{|\mathcal{N}_c|+1, \cdots, |\mathcal{N}_c|+|\mathcal{N}_d|\}$. $\mathcal{N}_d$ contains the sensor nodes that transmit their data to the sink directly, *i.e.*, their distances to the path are smaller than d_h, while $\mathcal{N}_c$ contains the sensor nodes that send data either directly or through a relay node. Define $\mathcal{R}_i$ as the set of candidate relay nodes of sensor node i. For any sensor node $j \in \mathcal{R}_i$, it must satisfy the following two conditions: 1)$j \in \mathcal{N}_d$, and 2) $d_{ij} \leq d_i^{tr}$, where d_{ij} is the distance between nodes i and j.

3.3. Data Transmission Model

Firstly, we introduce the data generation model at the sensor nodes. Similar to [38], $a_k(t)$ is defined as the sensing rate (i.e., the amount of data generated per time slot) of sensor node k at time slot t, which can be either a constant or a stochastic process. As $a_k(t)$ may not be supported by the limited network capability, each sensor node needs to control the stored data to keep its data buffer stable. We define the amount of data generated by node k and stored into its data buffer at time slot t as $x_k(t)$, and it satisfies $x_k(t) \in [0, a_k(t)]$.

[2]In this paper, we consider the constant distance threshold d_h. How to derive the optimal d_h is left as the future work.

Secondly, the time scheduling model is presented. Following the assumption in [30], in order to avoid data transmission collision, each time slot can be scheduled to only one transmission link. Then we define $\tau_{ij}(t) \in \{0,1\}$ as a binary time scheduling variable, and $\tau_{ij}(t) = 1$ indicates that time slot t is allocated to the link from nodes i to j. Thus, the time scheduling variables $\boldsymbol{\tau}(t) = \{\tau_{ij}(t), i \in \mathcal{K}, j \in \mathcal{N}_d \cup s\}$ satisfy

$$\begin{aligned}\boldsymbol{\tau}(t) \in \Lambda(t) = \Big\{ & \boldsymbol{\tau}(t) \mid \tau_{ks}(t)[\tau_{ks}(t)-1] = 0, \forall k \in \mathcal{K}, t \in [\underline{t}_k^{tr}, \bar{t}_k^{tr}]; \\ & \tau_{ks}(t) = 0, \forall k \in \mathcal{K}, t \notin [\underline{t}_k^{tr}, \bar{t}_k^{tr}]; \tau_{ij}(t)[\tau_{ij}(t)-1] = 0, \forall i \in \mathcal{N}_c, j \in \mathcal{R}_i; \\ & \tau_{ij}(t) = 0, \forall i \in \mathcal{N}_c, j \notin \mathcal{R}_i \text{ or } \forall i, j \in \mathcal{N}_d; \sum_{i \in \mathcal{K}} \sum_{j \in \mathcal{N}_d \cup s} \tau_{ij}(t) = 1 \Big\}, \end{aligned} \quad (1)$$

where $\Lambda(t)$ denotes the feasible set of $\boldsymbol{\tau}(t)$ at time slot t. $\sum_{i \in \mathcal{K}} \sum_{j \in \{\mathcal{N}_d \cup s\}} \tau_{ij}(t) = 1$ ensures that each time slot is allocated to only one transmission link, which is either from a sensor node to the sink or from a sensor node to its selected relay node. $\underline{t}_k^{tr}$ and $\bar{t}_k^{tr}$ denote the earliest and latest time slots that node k may directly send data to s respectively, which is derived by the following lemma.

Lemma 1. *For sensor node $k \in \mathcal{K}$, only when the sink s moves within its transmission region, namely $t \in [\underline{t}_k^{tr}, \bar{t}_k^{tr}]$, node k may directly transmit data to s. Thus, $\underline{t}_k^{tr}$ and $\bar{t}_k^{tr}$ can be given by*

$$\underline{t}_k^{tr} = \left\lceil \frac{\max\left\{x_k - \sqrt{(d_k^{tr})^2 - (y_k - y_0)^2}, 0\right\}}{v \cdot T} \right\rceil, \quad (2)$$

$$\bar{t}_k^{tr} = \left\lfloor \frac{\min\left\{x_k + \sqrt{(d_k^{tr})^2 - (y_k - y_0)^2}, v \cdot N \cdot T\right\}}{v \cdot T} \right\rfloor. \quad (3)$$

Observation 1: If the distance of sensor node k to the path is smaller, the time duration that the sink stays in its transmission region is longer, and thus the number of time slots that can be used for direct transmission is also larger.

Lastly, the transmission rate at the sensor nodes is introduced. Define $P_{ij}(t)$ and $e_{ij}(t)$ as the allocated power and consumed energy for data transmission on the link from node i to node j at the t-th time slot respectively, and $e_{ij}(t) = \tau_{ij}(t) P_{ij}(t) T$. Meanwhile, $r_{ij}(t)$ denotes the amount of data transmitted through the link from node i to node j, and $r_{ij}(t) \leq R\big(\tau_{ij}(t), P_{ij}(t), h_{ij}(t)\big)$,

where $R(\cdot)$ is rate function and $h_{ij}(t)$ is channel gain. In this paper, we use the shannon capacity as the rate function [31] such that $R\big(\tau_{ij}(t), P_{ij}(t), h_{ij}(t)\big) = \tau_{ij}(t)TW\log_2\big(1+\frac{P_{ij}(t)|h_{ij}(t)|^2}{(d_{ij}(t)/d_0)^{\alpha}L_0(d_0)N_0}\big)$, where W is the bandwidth, $(d_{ij}(t)/d_0)^{\alpha}$ $L_0(d_0)$ represents the path loss, and N_0 is the power of background noise.

For sensor node $i \in \mathcal{N}_c$, the amount of data added into its data buffer at time slot t is $x_i(t)$. As sensor node i may transmit data to either the sink or one of its relay nodes, the amount of data to be transmitted out of its data buffer equals $\sum_{j\in\mathcal{R}_i\cup s} r_{ij}(t)$. For sensor node $j \in \mathcal{N}_d$, which directly transmits data to the sink s, the amount of data added into its data buffer at time slot t includes its generated data and the data received from sensor nodes in $\mathcal{N}_c$. Thus, the amounts of received and transmitted data of sensor node j at time slot t are $x_j(t) + \sum_{i\in\mathcal{N}_c} r_{ij}(t)$ and $r_{js}(t)$, respectively.

3.4. Energy Harvesting and Consumption Model

To simplify the discussion, the energy consumption for receiving data is assumed to be negligible when compared to that of the sensing and transmitting operations, and we define a constant sensing energy consumption $\mathbf{e}_k^{sn}$ for sensor node k. According to the network and mobility model, at time slot t, the location of mobile sink is $(t\cdot v\cdot T, y_0)$. Thus we can derive the distance between sensor node k and the sink s at time slot t as $d_{ks}(t) = \sqrt{(x_k - t\cdot v\cdot T)^2 + (y_k - y_0)}$. Define $\underline{t}_k^e$ and $\overline{t}_k^e$ as the earliest and latest time slots when the sensor node k is in the energy transfer region respectively, and then it yields the following lemma.

Lemma 2. *Within the time slot $t \in [\underline{t}_k^e, \overline{t}_k^e]$, the sensor node k is in the energy transfer region of the mobile sink s, and $\underline{t}_k^e, \overline{t}_k^e$ satify,*

$$\underline{t}_k^e = \left\lceil \frac{\max\{x_k - \sqrt{d_e^2 - (y_k - y_0)^2}, 0\}}{v\cdot T} \right\rceil, \tag{4}$$

$$\overline{t}_k^e = \left\lfloor \frac{\min\{x_k + \sqrt{d_e^2 - (y_k - y_0)^2}, v\cdot N\cdot T\}}{v\cdot T} \right\rfloor. \tag{5}$$

Observation 2: If $|y_k - y_0|$ is larger, $\underline{t}_k^e$ and $\overline{t}_k^e$ are closer. Therefore, the sensor nodes that are farther away from the path always have less time duration for energy harvesting. In contrast, the sensor nodes closer to the path have more

time slots. Thus, the closer sensor nodes may allocate part of their harvested energy for forwarding data on behalf of the farther sensor nodes.

During the time slot $t \in [\underline{t}_k^e, \bar{t}_k^e]$, sensor node k is within the energy transfer region, and the amount of harvested energy is denoted by $e_k^h(t) = \frac{\eta P_s T |g_{sk}(t)|^2}{(d_{ks}(t)/d_0)^\alpha L_0(d_0)}$, where η is the energy conversion efficiency, P_s is the transmit power of the sink for charging the sensor nodes, $|g_{sk}(t)|^2$ is the channel gain from the sink to sensor node k in WET mode, and $(d_{ks}(t)/d_0)^\alpha L_0(d_0)$ is the path loss that depends on the distance. Thus, the energy harvested by all sensor nodes at time slot t can be denoted as $\boldsymbol{e}^h(t) = \left(e_1^h(t), \cdots, e_K^h(t)\right)$, and it satisfies:

$$\boldsymbol{e}^h(t) \in \Lambda_h(t) = \left\{ \boldsymbol{e}^h(t) \mid e_k^h(t) = \frac{\eta P_s T |g_{sk}(t)|^2}{(d_{ks}(t)/d_0)^\alpha L_0(d_0)},\ if\ t \in [\underline{t}_k^e, \bar{t}_k^e] \right\}, \quad (6)$$

where $\Lambda_h(t)$ denotes the feasible set of the amount of energy harvested at time slot t. We define $\boldsymbol{e}(t) = \{e_{ij}(t), \forall i \in \mathcal{K}, j \in \mathcal{N}_d \cup s\}$ as the energy consumed on all the links for data transmission, and it satisfies $\boldsymbol{e}(t) \in \Lambda_e(t) = \left\{ \boldsymbol{e}(t) \mid e_{ij}(t) = \tau_{ij}(t) P_{ij}(t) T \right\}$.

4. Joint Data Gathering and Energy Harvesting Scheduling

4.1. Problem Formulation

The network utility maximization (NUM) framework [16] has found many important applications in designing communication systems, especially in cross-layer resource allocation. In NUM, each source has a local utility function over its transmission rate, and it evaluates the value of its individual utility from the perspective of the whole network. The network utility is the sum of all local utilities. The utility function is usually a continuously differentiable, increasing and strictly concave function of the transmission rate. Two typical utility functions are linear functions, *i.e.*, $U(X_k) = X_k$, and logarithmic function, *i.e.*, $U(X_k) = \log_2(X_k)$, where X_k denotes the average transmission rate at node k. If $U(X_k) = X_k$, the network utility is equal to the total network throughput. While in the case of $U(X_k) = \log_2(X_k)$, since a low rate seriously affects the network utility, *i.e.*, $\lim_{X_k \to 0} U(X_k) = -\infty$, the logarithmic utility can provide better fairness, and has been widely adopted in the literature [30, 35, 38].

In this paper, we utilize the NUM framework to formulate the joint data gathering and energy harvesting (JoDGE) problem, and the logarithmic utility is adopted as it could simultaneously evaluate the throughput and fairness. The logarithmic utility is set to be $U(X_k) = \log_2(X_k)$, where $X_k = \frac{1}{N}\sum_{t=1}^{N} x_k(t)$ denotes the average amount of data stored at sensor node k in one pass. Meanwhile, X_k also defines the average transmission rate supported by the network, which also implies that the rate control guarantees the data buffer to be stable. Based on the energy and data transmission models, we formulate the JoDGE problem as follows,

$$
\begin{aligned}
\max \quad & \sum_{k\in\mathcal{K}} U\Big(\frac{1}{N}\sum_{t=1}^{N} x_k(t)\Big) \\
s.t. \quad & C1: \frac{1}{N}\sum_{t=1}^{N} x_i(t) \le \frac{1}{N}\sum_{t=1}^{N}\sum_{j\in\mathcal{R}_i\cup s} r_{ij}(t), \forall i \in \mathcal{N}_c, \\
& C2: \frac{1}{N}\sum_{t=1}^{N}\sum_{j\in\mathcal{R}_i\cup s} e_{ij}(t) \le \frac{1}{N}\sum_{t=1}^{N} e_i^h(t) - \mathbf{e}_i^{sn}, \forall i \in \mathcal{N}_c, \\
& C3: \frac{1}{N}\sum_{t=1}^{N}\Big[x_j(t) + \sum_{i\in\mathcal{N}_c} r_{ij}(t)\Big] \le \frac{1}{N}\sum_{t=1}^{N} r_{js}(t), \forall j \in \mathcal{N}_d, \\
& C4: \frac{1}{N}\sum_{t=1}^{N} e_{js}(t) \le \frac{1}{N}\sum_{t=1}^{N} e_j^h(t) - \mathbf{e}_j^{sn}, \forall j \in \mathcal{N}_d, \\
& C5: 0 \le x_k(t) \le a_k(t), 0 \le r_{ij}(t) \le R\big(\tau_{ij}(t), P_{ij}(t), h_{ij}(t)\big), \\
& \boldsymbol{\tau}(t) \in \Lambda(t), \boldsymbol{e}^h(t) \in \Lambda_h(t), \boldsymbol{e}(t) \in \Lambda_e(t), \forall k, i, j \in \mathcal{K}, \forall t.
\end{aligned}
\tag{7}
$$

Our goal is to derive an optimal scheduling scheme that jointly considers the power allocation, relay selection, and time slot scheduling problems. Constraints $C1$, $C2$, $C3$ and $C4$ are the stable and sustainable constraints of the data buffer and battery of each node respectively. For data buffer, the average amount of received data must be no larger than that of scheduled data in the network. For the battery, in order to ensure sustainable operations, the average consumed energy must be smaller than its average harvested energy. Constraint $C5$ defines the instantaneous feasible set to be satisfied at each time slot.

4.2. Problem Transformation

Problem (7) is a mixed integer nonlinear programming (MINLP) problem that is difficult to be solved directly. Thus, we transform it into a convex problem and then develop an *optimal joint data gathering and energy harvesting scheduling* (Opt-JoDGE) scheme. To achieve this goal, the following two steps will be performed: firstly, relaxing the mixed integer feasible set into a continuous feasible set; and secondly, converting the non-concave rate functions to concave functions based on the first step.

4.2.1. Time-sharing Relaxation

In problem (7), the binary variable vector $\boldsymbol{\tau}(t)$ is introduced by the time slot scheduling among all transmission links. Thus, the first step is to relax the binary variables to be a continuous feasible set. If $\tau_{ij}(t)$ is relaxed to be a continuous feasible set as $\tau_{ij}(t) \in [0,1]$, $\boldsymbol{\tau}(t)$ satisfies:

$$\begin{aligned}\boldsymbol{\tau}(t) \in \Lambda'(t) = \Big\{ & \boldsymbol{\tau}(t) \mid \tau_{ks}(t)[\tau_{ks}(t)-1] \leq 0, \forall k \in \mathcal{K}, t \in [\underline{t}_k^{tr}, \bar{t}_k^{tr}]; \\ & \tau_{ks}(t) = 0, \forall k \in \mathcal{K}, t \notin [\underline{t}_k^{tr}, \bar{t}_k^{tr}]; \tau_{ij}(t)[\tau_{ij}(t)-1] \leq 0, \forall i \in \mathcal{N}_c, j \in \mathcal{R}_i; \\ & \tau_{ij}(t) = 0, \forall i \in \mathcal{N}_c, j \notin \mathcal{R}_i \text{ or } \forall i, j \in \mathcal{N}_d; \sum_{i \in \mathcal{K}} \sum_{j \in \mathcal{N}_d \cup s} \tau_{ij}(t) = 1 \Big\}. \end{aligned} \quad (8)$$

By the relaxation, $\Lambda'(t)$ is a convex feasible set. Note that this relaxation has its corresponding physical meaning: multiple transmission links may share one time slot by splitting it into multiple sub-slots with different ratios. This can be considered as a time-sharing policy. In *Lemma* 3, we will derive that, for the primal problem (7), the optimal $\tau_{ij}^*(t)$ is always either 0 or 1. Therefore, the time-sharing mechanism is not necessary.

4.2.2. Analysis of Convexity

After the time-sharing relaxation, the problem is still non-convex due to the non-concave rate function $R\big(\tau_{ij}(t), P_{ij}(t), h_{ij}(t)\big)$. Fortunately, as $f(x,y) = x\ln(1+\frac{y}{x})$ is a concave function with respect to (x,y), we can easily derive that if $\tau_{ij}(t) \in [0,1]$, the rate function could be replaced by the equivalent rate function $R\big(\tau_{ij}(t), e_{ij}(t), h_{ij}(t)\big) = \tau_{ij}(t)TW\log_2\big(1+\frac{e_{ij}(t)|h_{ij}(t)|^2}{\tau_{ij}(t)T(d_{ij}(t)/d_0)^{\alpha}L_0(d_0)N_0}\big)$.

Thus, by the two steps and inserting $X_k = \frac{1}{N}\sum_{t=1}^{N} x_k(t)$, problem (7) can be transformed into the following convex problem:

$$\begin{aligned}
\max \quad & \sum_{k\in\mathcal{K}} U\Big(X_k\Big) \\
s.t. \quad & C1: X_i \le \frac{1}{N}\sum_{t=1}^{N}\sum_{j\in\mathcal{R}_i\cup s} r_{ij}(t), \forall i \in \mathcal{N}_c, \\
& C2: \frac{1}{N}\sum_{t=1}^{N}\sum_{j\in\mathcal{R}_i\cup s} e_{ij}(t) \le \frac{1}{N}\sum_{t=1}^{N} e_i^h(t) - \mathbf{e}_i^{sn}, \forall i \in \mathcal{N}_c, \\
& C3: X_j + \frac{1}{N}\sum_{t=1}^{N}\sum_{i\in\mathcal{N}_c} r_{ij}(t) \le \frac{1}{N}\sum_{t=1}^{N} r_{js}(t), \forall j \in \mathcal{N}_d, \\
& C4: \frac{1}{N}\sum_{t=1}^{N} e_{js}(t) \le \frac{1}{N}\sum_{t=1}^{N} e_j^h(t) - \mathbf{e}_j^{sn}, \forall j \in \mathcal{N}_d, \\
& C5: 0 \le X_k \le \bar{a}_k, 0 \le r_{ij}(t) \le R\big(\tau_{ij}(t), e_{ij}(t), h_{ij}(t)\big), \\
& \qquad \boldsymbol{\tau}(t) \in \Lambda'(t), \boldsymbol{e}^h(t) \in \Lambda_h(t), \boldsymbol{e}(t) \in \Lambda_e(t), \forall k, i, j \in \mathcal{K}, \forall t.
\end{aligned} \tag{9}$$

where $\bar{a}_k = \frac{1}{N}\sum_{t=1}^{N} a_k(t)$ denotes the average generation rate at sensor node k.

4.3. Optimal Joint Data Gathering and Energy Harvesting Scheduling Scheme

Since problem (9) is a standard convex problem, we can design an *optimal joint data gathering and energy harvesting scheduling* (Opt-JoDGE) scheme by employing dual decomposition and subgradient methods [4, 11].

Denote $\boldsymbol{\lambda} = (\lambda_1, \lambda_2, \cdots, \lambda_K)$ and $\boldsymbol{\nu} = (\nu_1, \nu_2, \cdots, \nu_K)$ as the lagrange multipliers associated with the stable and sustainable constraints, respectively. Thus the dual function is given as,

$$\begin{aligned}
\mathcal{L}(\boldsymbol{\lambda}, \boldsymbol{\nu}) = \min & -\sum_{k\in\mathcal{K}} U\big(X_k\big) + \sum_{i\in\mathcal{N}_c} \lambda_i \Big\{ X_i - \frac{1}{N}\sum_{t=1}^{N}\sum_{j\in\mathcal{R}_i\cup s} r_{ij}(t) \Big\} \\
& + \sum_{i\in\mathcal{N}_c} \nu_i \Big\{ \frac{1}{N}\sum_{t=1}^{N}\sum_{j\in\mathcal{R}_i\cup s} e_{ij}(t) - \frac{1}{N}\sum_{t=1}^{N} e_i^h(t) + \mathbf{e}_i^{sn} \Big\} \\
& + \sum_{j\in\mathcal{N}_d} \lambda_j \Big\{ X_j + \frac{1}{N}\sum_{t=1}^{N}\sum_{i\in\mathcal{N}_c} r_{ij}(t) - \frac{1}{N}\sum_{t=1}^{N} r_{js}(t) \Big\} \\
& + \sum_{j\in\mathcal{N}_d} \nu_j \Big\{ \frac{1}{N}\sum_{t=1}^{N} e_{js}(t) - \frac{1}{N}\sum_{t=1}^{N} e_j^h(t) + \mathbf{e}_j^{sn} \Big\}.
\end{aligned} \tag{10}$$

Given $\boldsymbol{\lambda}$ and $\boldsymbol{\nu}$, (10) is further sub-divided into two independent problems as,

$$\mathcal{L}_1(\boldsymbol{\lambda},\boldsymbol{\nu}) = \min_{X_k\in[0,\bar{a}_k],\forall k\in\mathcal{K}} -\sum_{k\in\mathcal{K}} U\big(X_k\big) + \sum_{i\in\mathcal{N}_c}\lambda_i X_i + \sum_{j\in\mathcal{N}_d}\lambda_j X_j, \tag{11}$$

$$\begin{aligned}\mathcal{L}_2(\boldsymbol{\lambda},\boldsymbol{\nu}) = \min \quad & \frac{1}{N}\sum_{t=1}^{N}\Big\{-\sum_{i\in\mathcal{N}_c}\lambda_i\sum_{j\in\mathcal{R}_i\cup s} r_{ij}(t) + \sum_{i\in\mathcal{N}_c}\nu_i\Big[\sum_{j\in\mathcal{R}_i} e_{ij}(t) \\ & - e_i^h(t) + \mathbf{e}_i^{sn}\Big] + \sum_{j\in\mathcal{N}_d}\lambda_j\Big[\sum_{i\in\mathcal{N}_c} r_{ij}(t) - r_{js}(t)\Big] \\ & + \sum_{j\in\mathcal{N}_d}\nu_j\Big[e_{js}(t) - e_j^h(t) + \mathbf{e}_j^{sn}\Big]\Big\}.\end{aligned} \tag{12}$$

For problem (11), by inserting $U(X_k) = \log_2(X_k)$ and taking derivative of X_k, the average data transmission rate of sensor node k can be given as

$$X_k = \frac{1}{N}\sum_{t=1}^{N} x_k(t) = \min\big\{\bar{a}_k, \frac{1}{\lambda_k \ln 2}\big\}, \tag{13}$$

where $\bar{a}_k$ represents the average data generation rate of sensor node k. Meanwhile, the objective function of problem (12) is the sum of N sub-functions, and each of them is associated with the variables at one individual time slot, *i.e.*, the t-th sub-function depends only on the variables $\boldsymbol{\tau}(t), \boldsymbol{e}(t), \mathbf{r}(t)$. Thus the problem can be decomposed into N sub-problems, and each sub-problem is related to one time slot, *i.e.*, the sub-problem at time slot t can be written as,

$$\begin{aligned}\min \quad & -\sum_{i\in\mathcal{N}_c}\sum_{j\in\mathcal{R}_i}[\lambda_i - \lambda_j] r_{ij}(t) - \sum_{k\in\mathcal{K}}\lambda_k r_{ks}(t) + \sum_{i\in\mathcal{N}_c}\sum_{j\in\mathcal{R}_i}\nu_i e_{ij}(t) \\ & + \sum_{k\in\mathcal{K}}\nu_j\big[e_{ks}(t) - e_k^h(t) + \mathbf{e}_k^{sn}\big] \\ s.t. \quad & 0 \le r_{ij}(t) \le R\big(\tau_{ij}(t), e_{ij}(t), h_{ij}(t)\big), \forall i,j\in\mathcal{K} \\ & \boldsymbol{\tau}(t) \in \Lambda'(t).\end{aligned} \tag{14}$$

In fact, the objective takes both the transmission rate and energy consumption into consideration, and it aims to achieve larger weighted rate with less weighted energy consumption, where the weights are dependent on $\boldsymbol{\lambda}$ and $\boldsymbol{\nu}$.

The first step is to determine the optimal transmission rate $\mathbf{r}(t)$. If $\lambda_i \le \lambda_j$, it yileds $r_{ij}(t) = 0$. Given $X_k = \min\big\{\bar{a}_k, \frac{1}{\lambda_k \ln 2}\big\}$, $\lambda_i \le \lambda_j$ always implies that

the data transmission rate of node j is less than that of node i, and it can be stated as: for node $j \in \mathcal{N}_d$, if it is a relay node, it must guarantee its own transmission rate first before helping other nodes to forward data. Based on this observation, we denote $\mathcal{R}'_i$ as the set of real relay nodes of node i. Thus $\mathcal{R}'_i = \{j|\lambda_i > \lambda_j, \forall i \in \mathcal{N}_c, j \in \mathcal{R}_i\}$. When $j \in \mathcal{R}'_i$, the optimal transmission rate on the link from node i to node j is denoted as $r^*_{ij}(t) = R\big(\tau_{ij}(t), e_{ij}(t), h_{ij}(t)\big)$. Then, by inserting the optimal transmission rate $\mathbf{r}^*(t)$ into problem (14), the energy/power allocation problem is given as,

$$\begin{aligned}\min_{\boldsymbol{e}(t),\boldsymbol{\tau}(t)} \; & -\sum_{i\in\mathcal{N}_c}\sum_{j\in\mathcal{R}'_i}[\lambda_i-\lambda_j]R\big(\tau_{ij}(t),e_{ij}(t),h_{ij}(t)\big)+\sum_{i\in\mathcal{N}_c}\sum_{j\in\mathcal{R}'_i}\nu_i e_{ij}(t)\\ & -\sum_{k\in\mathcal{K}}\lambda_k R\big(\tau_{ks}(t),e_{ks}(t),h_{ks}(t)\big)+\sum_{k\in\mathcal{K}}\nu_k\big[e_{ks}(t)-e^h_j(t)+\mathbf{e}^{sn}_j\big] \qquad (15)\\ s.t. \quad & \boldsymbol{\tau}(t)\in\Lambda'(t), \boldsymbol{e}(t)\in\Lambda_e(t).\end{aligned}$$

where $R\big(\tau_{ij}(t), e_{ij}(t), h_{ij}(t)\big) = \tau_{ij}(t)TW\log_2\Big(1+\frac{e_{ij}(t)|h_{ij}(t)|^2}{\tau_{ij}(t)T(d_{ij}(t)/d_0)^\alpha L_0(d_0)N_0}\Big)$. Since each term is associated with only one energy allocation variable, the problem can be further decomposed. For example, to derive the allocated energy $e_{ij}(t)$, we only need to solve the following problem,

$$\min_{e_{ij}(t)} \; -[\lambda_i-\lambda_j]\tau_{ij}(t)TW\log_2\Big(1+\frac{e_{ij}(t)|h_{ij}(t)|^2}{\tau_{ij}(t)T(d_{ij}(t)/d_0)^\alpha L_0(d_0)N_0}\Big)+\nu_i e_{ij}(t). \qquad (16)$$

By taking derivative with respect to $e_{ij}(t)$, this problem can be solved easily. Similar procedure can be applied to variable $e_{ks}(t), \forall k \in \mathcal{K}$. Thus we can derive the optimal energy allocation scheme.

Theorem 1. *For the link between sensor node $i \in \mathcal{N}_c$, and the corresponding relay node $j \in \mathcal{R}'_i$, the optimal allocated energy is given as*

$$e^*_{ij}(t) = \tau_{ij}(t)TP^*_{ij}(t) = \tau_{ij}(t)T\Big[\frac{\lambda_i-\lambda_j}{\ln 2\cdot\nu_i}-\frac{(d_{ij}(t)/d_0)^\alpha L_0(d_0)N_0}{|h_{ij}(t)|}\Big]^\dagger, \qquad (17)$$

where $[x]^\dagger = \max\{0, x\}$, and $P^*_{ij}(t)$ represents the optimal allocated power. For sensor node $k \in \mathcal{K}$ that directly transmits data to the sink, the optimal allocated energy can be written as

$$e^*_{ks}(t) = \tau_{ks}(t)TP^*_{ks}(t) = \tau_{ks}(t)T\Big[\frac{\lambda_k}{\ln 2\cdot\nu_k}-\frac{(d_{ks}(t)/d_0)^\alpha L_0(d_0)N_0}{|h_{ks}(t)|}\Big]^\dagger. \qquad (18)$$

Observation 3: The optimal energy/power allocation scheme complies with the traditional *water-filling* mechanism [13]. As is shown in (17) and (18), the optimal power consists of two terms. The first term is associated with lagrange multipliers $\boldsymbol{\lambda}$ and $\boldsymbol{\nu}$, and the second term depends on the channel gain and transmission distance. For the second term, the optimal power allocation scheme is a *water-filling* mechanism over the link condition. If the state is better, the second part is smaller and the transmitter can allocate more power to achieve a higher transmission rate. Otherwise, it consumes less power to avoid the waste of power/energy in the poor channel condition.

Lastly, the time scheduling problem needs to be solved. By inserting the optimal energy allocation scheme, problem (15) can be rewritten as,

$$\begin{aligned}\min_{\boldsymbol{\tau}(t)} & -\sum_{i\in\mathcal{N}_c}\sum_{j\in\mathcal{R}_i}[\lambda_i-\lambda_j]\tau_{ij}(t)R^*_{ij}(t)-\sum_{k\in\mathcal{K}}\lambda_k\tau_{ks}(t)R^*_{ks}(t)\\ &+\sum_{i\in\mathcal{N}_c}\sum_{j\in\mathcal{R}'_i}\nu_i\tau_{ij}(t)P^*_{ij}(t)+\sum_{k\in\mathcal{K}}\nu_k\big[\tau_{ks}(t)P^*_{ks}(t)-e^h_j(t)+\mathbf{e}^{sn}_j\big],\end{aligned} \tag{19}$$

where $R^*_{ij}(t)=TW\log_2\big(1+\frac{P^*_{ij}(t)|h_{ij}(t)|^2}{(d_{ij}(t)/d_0)^{\varepsilon}L_0(d_0)N_0}\big)$. (19) is a linear programming problem, and thus the optimal time slot scheduling variable $\tau_{ij}(t)$ is either 1 or 0. Since (9) is the relaxed problem of (7) by enlarging the feasible set, the optimal solution of (9) is an upper bound of that of (7). Since we observe that the optimal solution of (9) also satisfies the constraints of (7), it is also the optimal solution of (7). Finally, the following lemma can be derived.

Lemma 3. *The optimal scheduling variable $\tau_{ij}(t)$ is either 1 or 0. For the optimal time slot scheduling, time-sharing is not necessary, and it only needs to allocate one time slot for one transmission link. Thus, the optimal solution for problem* (9) *is also a feasible and optimal solution of problem* (7)*.*

As the optimal value for $\tau_{ij}(t)$ is either 1 or 0, and there are finite links, problem (19) can be solved by exhaustive search. Firstly, for sensor node $i\in\mathcal{N}_c$, it selects the "best" transmission links among all links to its relay nodes and the sink, which achieves the highest weighted transmission rate with the least weighted energy consumption. This procedure can be considered as the relay

selection. Secondly, for all sensor nodes $k \in \mathcal{K}$, the time scheduling scheme is to schedule the best sensor node to transmit data on its "best" link. The following two theorems present the relay selection scheme and time scheduling scheme, respectively.

Theorem 2. *For sensor node $i \in \mathcal{N}_c$, the destination node is either the sink or one of its relay nodes. The selected destination node is S_i, namely, relay selection policy, and it satisfies,*

$$S_i = \arg\max_j A_i \tag{20}$$

where $A_i = \left(A_{i\mathcal{N}_c+1}, \cdots, A_{iK}, A_{is}\right)$ and A_{ij} is the scheduling reward that is the weighted transmission rate minus the weighted energy consumption as follows,

$$A_{ij} = \begin{cases} [\lambda_i - \lambda_j] f_{ij}^*(t) - \nu_i P_{ij}^*(t) T, & \text{if j} \in \mathcal{R}_\text{i}' \\ \lambda_i f_{is}^*(t) - \nu_i P_{ij}^*(t) T, & \text{if j} = \text{s}, \\ -\infty, & \text{otherwise.} \end{cases} \tag{21}$$

Theorem 3. *The time slot scheduling scheme is to determine at each time slot which sensor node is going to transmit data to a selected relay node or the sink. Define the scheduling reward vector $B = (B_1, B_2, \cdots, B_K)$, where $B_k = max_j A_i, \forall k \in \mathcal{N}_c$, and $B_k = \lambda_k f_{ks}^*(t) - \nu_i P_{ks}^*(t) T, \forall j \in \mathcal{N}_d$, the optimal time slot scheduling scheme is to choose the "best" transmission link with the largest scheduling reward, and can be given as*

$$\tau_{ij}^*(t) = \begin{cases} 1, & \text{if } i = \arg\max_k B \text{ and } \{i \in \mathcal{N}_c, j = S_i \text{ or } i \in \mathcal{N}_d, j = s\}, \\ 0, & \text{otherwise.} \end{cases} \tag{22}$$

Another critical issue is how to derive the Lagrange multipliers $\boldsymbol{\lambda} = \left(\lambda_1, \lambda_2, \cdots, \lambda_K\right)$ and $\boldsymbol{\nu} = \left(\nu_1, \nu_2, \cdots, \nu_K\right)$. Since problem (9) is a standard convex problem, based on the KKT (Karush-Kuhn-Tucker) condition, the Lagrange multipliers must be satisfied so that the stable and sustainable constraints $C1$, $C2$, $C3$ and $C4$ hold with equality. Even though this characteristic exists, it is still difficult to derive their closed form expressions, and some numerical methods such as the sub-gradient method [4, 11] are usually adopted.

5. Near-Optimal Buffer-Battery-Aware Scheduling

The Opt-JoDGE scheme proposed in Section 4 depends on the Lagrange multipliers, whose closed form expressions are not easy to be derived. Furthermore, the run-time status of the data buffer and battery are not considered. In this section, we introduce the *Near-Optimal Buffer-Battery-Aware Adaptive scheduling (NO-BBA)* scheme, which also exploits the run-time status of the data buffer and battery of individual sensor node, to derive the relationship between the average buffer size and the network performance. Meanwhile, some implementation issues and special cases are also discussed.

5.1. Problem Formulation

Denote $\mathbf{Q}_k(t)$ as the status of the data buffer of sensor node k at time slot t. Based on the data transmission model as specified in Section 3.3, the evolution expressions of the status of data buffer at node i and node j, $(i \in \mathcal{N}_c, j \in \mathcal{N}_d)$, are presented as follows:

$$\mathbf{Q}_i(t+1) = \Big[\mathbf{Q}_i(t) - \textstyle\sum_{j\in\mathcal{R}_i\cup s} r_{ij}(t)\Big]^{\dagger} + x_i(t), \forall i \in \mathcal{N}_c, \tag{23}$$

$$\mathbf{Q}_j(t+1) = \Big[\mathbf{Q}_j(t) - r_{js}(t)\Big]^{\dagger} + x_j(t) + \textstyle\sum_{i\in\mathcal{N}_c} r_{ij}(t), \forall j \in \mathcal{N}_d. \tag{24}$$

In order to monitor the environment continuously, it is assumed that sensor node k consumes $\mathbf{e}_k^{sn}$ energy at each time slot for sensing operations. The sensor nodes should not consume all the energy in their batteries for data transmission, and should reserve sufficient amount of energy for sensing operations in the future. For this purpose, we divide the battery of each sensor node into two virtual sub-batteries: the first one is to store harvested energy for sensing operations while the second one is for data transmission. In order to guarantee sustainable sensing of the environment, we adopt the following energy reservation policy: at the beginning of each pass, the first sub-battery stores sufficient energy for sensing operations in the current pass, usually no less than $N\mathbf{e}_k^{sn}$. Therefore, when a sensor node harvests energy, it first supplements the first sub-battery to reserve enough sensing energy for the next pass. The remaining harvested energy is to charge the second sub-battery for data transmission.

We use $\mathbf{E}_k^{sn}(t)$ to denote the amount of energy to be harvested for sensing operations in the first sub-battery of sensor node k at time slot t. At the beginning of each pass, $\mathbf{E}_k^{sn}(t)$ is set to be $N\mathbf{e}_k^{sn}$, *i.e.* $\mathbf{E}_k^{sn}(mN+1) = N\mathbf{e}_k^{sn}$. Thus the evolution expression of $\mathbf{E}_k^{sn}(t)$ can be written as $\mathbf{E}_k^{sn}(t+1) = \max\{\mathbf{E}_k^{sn}(t) - e_k^h(t), 0\} = \mathbf{E}_k^{sn}(t) - \ddot{e}_k^h(t)$, where $\ddot{e}_k^h(t) = \min\{\mathbf{E}_k^{sn}(t), e_k^h(t)\}$. $e_k^h(t)$ represents the energy harvested by sensor node k at time slot t, and $\ddot{e}_k^h(t)$ is the actual amount of energy replenished into the first sub-battery. At each time slot, after replenishing the first sub-battery, the remaining harvested energy will be stored into the second sub-battery. Thus at time slot t the energy stored for data transmission can be denoted as $\widetilde{e}_k^h(t)$, which satisfies $\widetilde{e}_k^h(t) = e_k^h(t) - \ddot{e}_k^h(t)$.

As the above energy reservation policy can guarantee the energy consumption of sensing operations, we thus ignore the first sub-battery and only consider the harvested and consumed energy for data transmission. Therefore, in the followings, we use the term "battery" to represent the second sub-battery.

Denote $\mathbf{E}_k(t)$ as the battery status of sensor node k at time slot t. Based on the energy harvesting and consumption model, the evolution equations of the battery of sensor nodes i and j, $(i \in \mathcal{N}_c, j \in \mathcal{N}_d)$, are presented as follows:

$$\mathbf{E}_i(t+1) = \mathbf{E}_i(t) - \sum_{j \in \mathcal{R}_i \cup s} e_{ij}(t) + \widetilde{e}_i^h(t), \forall i \in \mathcal{N}_c, \tag{25}$$

$$\mathbf{E}_j(t+1) = \mathbf{E}_j(t) - e_{js}(t) + \widetilde{e}_j^h(t), \forall j \in \mathcal{N}_d, \tag{26}$$

where $\widetilde{e}_i^h(t)$ (or $\widetilde{e}_j^h(t)$) and $\sum_{j \in \mathcal{R}_i \cup s} e_{ij}(t)$ (or $e_{js}(t)$) represent the harvested and consumed energy by sensor node i (or j) at time slot t, respectively.

The goal of the buffer-battery-aware scheduling is to maximize network utility under the stability constraint of the data buffer and sustainable constraint of the battery at each sensor node. Here, the stability constraint of data buffer specifies that the amount of buffered data should not approach to infinity when $t \to \infty$, and the sustainable constraint of battery requires that the average harvested energy must be no less than the average consumed energy for both data transmission and sensing operations, namely, $\frac{1}{N}\sum_{t=1}^{N}\sum_{j \in \mathcal{N}_d \cup s}\mathbb{E}[e_{kj}(t)] \leq \frac{1}{N}\sum_{t=1}^{N}\mathbb{E}[e_k^h(t)] - \mathbf{e}_k^{sn}$. As $\widetilde{e}_k^h(t) = e_k^h(t) - \ddot{e}_k^h(t)$, we have $\frac{1}{N}\sum_{t=1}^{N}\mathbb{E}[e_k^h(t)] =$

$\frac{1}{N}\sum_{t=1}^{N}\mathbb{E}[\widetilde{e}_k^h(t)]+\frac{1}{N}\sum_{t=1}^{N}\mathbb{E}[\ddot{e}_k^h(t)]$. According to the energy reservation policy, we can find that the energy supplied to the first sub-battery in one pass is equal to $N\mathbf{e}_k^{sn}$, *i.e.*, $\frac{1}{N}\sum_{t=1}^{N}\mathbb{E}[\ddot{e}_k^h(t)]=\mathbf{e}_k^{sn}$. Thus, we can derive an equivalent form of sustainable constraint as follows,

$$\frac{1}{N}\sum_{t=1}^{N}\sum_{j\in\mathcal{N}_d\cup s}\mathbb{E}[e_{kj}(t)]\leq\frac{1}{N}\sum_{t=1}^{N}\mathbb{E}[\widetilde{e}_k^h(t)],\forall k\in\mathcal{K}, \tag{27}$$

which only considers the harvested and consumed energy of the second sub-battery.

Proposition 1. *For any queue $q(t)$ with evolution $q(t+1)=\big(q(t)-u(t)\big)^{\dagger}+\lambda(t)$, where $u(t)$ and $\lambda(t)$ represents the departure and arrival processes, respectively. If the queue $q(t)$ is mean rate stable,* i.e., $\limsup_{N\to\infty}\frac{\mathbb{E}[q(N)]}{N}=0$, *we have* $\limsup_{N\to\infty}\frac{1}{N}\sum_{t=0}^{N-1}\big\{\mathbb{E}[\lambda(t)]-\mathbb{E}[u(t)]\big\}\leq 0$, *which indicates that the average arrival process is no larger than the average departure process.*

This proposition is similar to *Theorem* 2.5 in [27] and the proof procedure is omitted here. With *Proposition* 1, the constraint in (27) can be converted to the stability constraint of a queue. Therefore, we can construct an energy queue, in which the consumed energy $\sum_{j\in\mathcal{N}_d\cup s}e_{kj}(t)$ and the harvested energy $\widetilde{e}_k^h(t)$ are the arrival and departure process, respectively. Comparing with the evolution equations of the battery in (25) and (26), the constructed energy queue is contrary to the battery, and thus we use $\phi_k-\mathbf{E}_k(t)$ to denote the constructed energy queue for sensor node k, and the evolution equation can be given by

$$\phi_k-\mathbf{E}_k(t+1)=\phi_k-\mathbf{E}_k(t)-\widetilde{e}_k^h(t)+\sum_{j\in\mathcal{N}_d\cup s}e_{kj}(t). \tag{28}$$

Here, the energy queue $\phi_k-\mathbf{E}_k(t)$ can be stated as vacant battery, in which the constant ϕ_k can be considered as the "virtual" capacity of the battery, and $\phi_k-\mathbf{E}_k(t)$ is the remaining space of the battery. A larger $\phi_k-\mathbf{E}_k(t)$ implies less stored energy in the battery.

5.2. Near-Optimal Buffer-Battery-Aware Adaptive Scheduling Scheme

We use $\mathbf{\Theta}(t)=\big[\mathbf{Q}_1(t),\cdots,\mathbf{Q}_K(t);\phi_1-\mathbf{E}_1(t),\cdots,\phi_K-\mathbf{E}_K(t)\big]$ to denote the generalized queue, which consists of all data buffers and energy queues. We

then introduce the quadratic Lyapunov function $\boldsymbol{L}\big(\boldsymbol{\Theta}(t)\big) = \frac{1}{2}\sum_{k\in\mathcal{K}} \mathbf{Q}_k(i)^2 + \frac{1}{2}\sum_{k\in\mathcal{K}} \mu_k\big[\phi_k - \mathbf{E}_k(i)\big]^2$ as similar as recommended in [27], where μ_k is a non-negative control parameter to characterize the relative effect of the data buffer and energy queue on the scheduling scheme, mainly to ensure that the first item and second item are in the same order of magnitude. Then, we can define the one-slot conditional Lyapunov Drift $\boldsymbol{\Delta}\big(\boldsymbol{\Theta}(t)\big) = \mathbb{E}\big[\boldsymbol{L}\big(\boldsymbol{\Theta}(t+1)\big) - \boldsymbol{L}\big(\boldsymbol{\Theta}(t)\big)|\boldsymbol{\Theta}(t)\big]$. This drift characterizes the expected changes in the Lyapunov function over one time slot, and reflects the increment of the generalized queue.

Combined with data transmission, we have the *drift-plus-penalty* as $\boldsymbol{\Delta}\big(\boldsymbol{\Theta}(t)\big) - V\sum_{k\in\mathcal{K}} U\big\{\mathbb{E}[x_k(t)|\boldsymbol{\Theta}(t)]\big\}$, where V is a non-negative control parameter that is chosen to quantify the tradeoff of queue backlog (first term) and average achievable performance (second term). If the channel gain is i.i.d over different time slots, the *drift-plus-penalty* is upper bounded as follows,

$$\begin{aligned}
\boldsymbol{\Delta}\big(\boldsymbol{\Theta}(t)\big) - V\sum_{k\in\mathcal{K}} \log_2\big(\mathbb{E}\big[x_k(t)|\boldsymbol{\Theta}(t)\big]\big) \leq B - \sum_{k\in\mathcal{K}} \Big\{ V\log_2\big(\mathbb{E}\big[x_k(t)|\boldsymbol{\Theta}(t)\big]\big) \\
- \mathbf{Q}_k(t)\mathbb{E}\big[x_k(t)|\boldsymbol{\Theta}(t)\big]\Big\} - \sum_{i\in\mathcal{N}_c}\sum_{j\in\mathcal{R}_i}\Big\{\big[\mathbf{Q}_i(t) - \mathbf{Q}_j(t)\big]\mathbb{E}\big[r_{ij}(t)|\boldsymbol{\Theta}(t)\big] \\
- \mu_i\big[\phi_i - \mathbf{E}_i(t)\big]\mathbb{E}\big[e_{ij}(t)|\boldsymbol{\Theta}(t)\big]\Big\} - \sum_{k\in\mathcal{K}}\Big\{\mathbf{Q}_k(t)\mathbb{E}\big[r_{ks}(t)|\boldsymbol{\Theta}(t)\big] \\
- \mu_k\big[\phi_k - \mathbf{E}_k(t)\big]\mathbb{E}\big[e_{js}(t)|\boldsymbol{\Theta}(t)\big]\Big\} - \sum_{k\in\mathcal{K}} \mu_k\big[\phi_k - \mathbf{E}_k(t)\big]\mathbb{E}\big[\widetilde{e}_k^h(t)|\boldsymbol{\Theta}(t)\big],
\end{aligned} \tag{29}$$

where $\boldsymbol{B}$ is a finite constant independent of V and given by,

$$\begin{aligned}
\boldsymbol{B} \geq \frac{1}{2}\sum_{i\in\mathcal{N}_c}\Big\{\mathbb{E}\big\{[x_i(t)]^2|\boldsymbol{\Theta}(t)\big\} + \mathbb{E}\big\{[\sum_{j\in\mathcal{R}_i\cup s} r_{ij}(t)]^2|\boldsymbol{\Theta}(t)\big\} \\
+ \mu_i\mathbb{E}\big\{[\sum_{j\in\mathcal{R}_i\cup s} e_{ij}(t)]^2|\boldsymbol{\Theta}(t)\big\} + \mu_i\mathbb{E}\big\{[\widetilde{e}_i^h(t)]^2|\boldsymbol{\Theta}(t)\big\}\Big\} \\
+ \frac{1}{2}\sum_{j\in\mathcal{N}_d}\Big\{\mathbb{E}\big\{[x_j(t) + \sum_{i\in\mathcal{N}_c} r_{ij}(t)]^2|\boldsymbol{\Theta}(t)\big\} + \mathbb{E}\big\{[r_{js}(t)]^2|\boldsymbol{\Theta}(t)\big\} \\
+ \mu_j\mathbb{E}\big\{[e_{js}(t)]^2|\boldsymbol{\Theta}(t)\big\} + \mu_j\mathbb{E}\big\{[\widetilde{e}_j^h(t)]^2|\boldsymbol{\Theta}(t)\big\}\Big\}.
\end{aligned} \tag{30}$$

Here, the procedure to derive the upper bound is similar to *Lemma* 4.6 in [27].

In order to keep the involved buffer stable and satisfy the energy constraints, we try to minimize the increment of the queue size. Meanwhile, in terms of effec-

tive transmission, we need to maximize the rate of data transmission. All these encourage us to minimize the *drift-plus-penalty*. Instead of directly minimizing the *drift-plus-penalty* item, our scheduling scheme actually seeks to minimize the upper bound in (29). At each time slot t, given the channel and queue status, the *Near-Optimal Buffer-Battery Aware Adaptive Scheduling* (NO-BBA) scheme can be utilized to solve the following optimization problem:

$$\begin{aligned}\max & \sum_{k\in\mathcal{K}}[V\log_2(x_k(t))-\mathbf{Q}_k(t)x_k(t)]+\sum_{i\in\mathcal{N}_c}\sum_{j\in\mathcal{R}_i}\Big\{\big[\mathbf{Q}_i(t)-\mathbf{Q}_j(t)\big]r_{ij}(t)\\ & -\mu_i\big[\phi-\mathbf{E}_i(t)\big]e_{ij}(t)\Big\}+\sum_{k\in\mathcal{K}}\Big\{\mathbf{Q}_k(t)r_{ks}(t)-\mu_k\big[\phi-\mathbf{E}_k(t)\big]e_{ks}(t)\Big\} \qquad (31)\\ s.t.\ & 0\le r_{ij}(t)\le R_{ij}(\tau_{ij}(t),P_{ij}(t),h_{ij}(t)),x_k(t)\in[0,a_k(t)],\\ & \boldsymbol{\tau}(t)\in\Lambda(t),\forall k\in\mathcal{K},i\in\mathcal{K},j\in\mathcal{N}_d\cup s.\end{aligned}$$

Observation 5: In problem (31), only the first term of the objective function is associated with $x_k(t)$. Therefore, the optimization of $x_k(t)$ can be decomposed, and considered as the rate control problem to control the amount of arrived data. The second and third terms have similar format, and they can be regarded as choosing the "best" link that achieves a higher weighted transmission rate with less weighted energy consumption, where the weighted values are dependent on their corresponding status of the data buffer and energy queue.

By solving problem (31), we can derive the following scheduling algorithm.

1. **Rate Control:** For any sensor node k, the rate control problem decides the amount of data to be added into the data buffer at each time slot t, namely, $x_k(t)=\min\big\{a_k(t),\frac{V}{\ln 2\cdot\mathbf{Q}_k(t)}\big\}$.

2. **Joint Power Allocation and Relay Selection for sensors in $\mathcal{N}_c$:**

   First of all, the rate variables $\mathbf{r}(t)$ are optimized. When $\mathbf{Q}_i(t)\ge\mathbf{Q}_j(t)$, we have $r_{ij}(t)=\tau_{ij}(t)TW\log_2\left(1+\frac{e_{ij}(t)|h_{ij}(t)|^2}{\tau_{ij}(t)T(d_{ij}/d_0)L_0(d_0)N_0}\right)$, otherwise $r_{ij}(t)=0$. This indicates that sensor node j could become a candidate relay node only in the case with smaller data buffer size.

   Secondly, by inserting $r_{ij}(t)$, the power allocation scheme can be easily

derived as follows,

$$P_{ij}^*(t) = \min\left\{\Big[\frac{\big[\mathbf{Q}_i(t) - \mathbf{Q}_j(t)\big]}{\ln 2\mu_i\big[\phi_i - \mathbf{E}_i(t)\big]} - \frac{(d_{ij}/d_0)^\alpha L_0(d_0)N_0}{|h_{ij}(t)|}\Big]^\dagger, \frac{\mathbf{E}_i(t)}{T}\right\}, \tag{32}$$

$$P_{is}^*(t) = \min\left\{\Big[\frac{\mathbf{Q}_i(t)}{\ln 2\mu_i\big[\phi_i - \mathbf{E}_i(t)\big]} - \frac{(d_{is}(t)/d_0)^\alpha L_0(d_0)N_0}{|h_{is}(t)|}\Big]^\dagger, \frac{\mathbf{E}_i(t)}{T}\right\}. \tag{33}$$

Lastly, the relay selection problem is to select the "best" link among the links from sensor node i to all its relay nodes and the sink. S_i denotes the destination of the selected link, and it can be given as

$$S_i = \arg\max A_i, \tag{34}$$

where $A_i = \big(A_{i\mathcal{N}_c+1}, \cdots, A_{iK}, A_{is}\big)$. A_{ij} represents the scheduling reward on the link from node i to node j, and it can be computed by the weighted transmission rate minus the weighted energy consumption as follows,

$$A_{ij} = \begin{cases} [\mathbf{Q}_i(t) - \mathbf{Q}_j(t)]f_{ij}^*(t) - \mu_i\big[\phi_i - \mathbf{E}_i(t)\big]P_{ij}^*(t)T, & \text{if j} \in \mathcal{R}_\text{i}' \\ \mathbf{Q}_i(t)f_{is}^*(t) - \mu_i\big[\phi_i - \mathbf{E}_i(t)\big]P_{ij}^*(t)T, & \text{if j} = \text{s}, \\ -\infty, & \text{otherwise}, \end{cases} \tag{35}$$

where $f_{ij}^*(t) = TW\log_2\big(1 + \frac{P_{ij}^*(t)|h_{ij}(t)|^2}{(d_{ij}(t)/d_0)^\alpha L_0(d_0)N_0}\big)$ denotes the amount of data bits transmitted from node i to node j.

3. **Power Allocation for sensors in $\mathcal{N}_d$:** Since only the third term of the objective function in (31) is associated with $e_{js}(t)$ (namely $\tau_{js}(t)TP_{js}(t)$), the corresponding power allocation scheme for sensor node $j \in \mathcal{N}_d$ can be easily derived as follows,

$$P_{js}^*(t) = \min\left\{\Big[\frac{\mathbf{Q}_j(t)}{\ln 2\mu_j\big[\phi_j - \mathbf{E}_j(t)\big]} - \frac{(d_{js}(t)/d_0)^\alpha L_0(d_0)N_0}{|h_{js}(t)|}\Big]^\dagger, \frac{\mathbf{E}_j(t)}{T}\right\}. \tag{36}$$

4. **Time-slot scheduling:** The time scheduling scheme is to allocate the time slots to the sensor nodes with the "best" links, which achieves the

largest weighted transmission rate by consuming the least weighted energy, and is stated as:

$$\tau_{ij}^{*}(t)=\begin{cases}1, & \text{if } i=\arg\max_k B \text{ and } \{i\in\mathcal{N}_c, j=S_i \text{ or } i\in\mathcal{N}_d, j=s\},\\ 0, & \text{otherwise,}\end{cases} \tag{37}$$

where $B=(B_1,B_2,\cdots,B_K)$ denotes the scheduling reward vector, and $B_i=A_{S_i},\forall i\in\mathcal{N}_c$, $B_j=\mathbf{Q}_j(t)f_{js}^{*}(t)-\mu_j\big[\phi_j-\mathbf{E}_j(t)\big]P_{js}^{*}(t)T,\forall j\in\mathcal{N}_d$.

Observation 6: For the rate control policy, $x_k(t)$ not only depends on the amount of generated data $a_k(t)$, but also relies on the status of the data buffer $\mathbf{Q}_k(t)$. This indicates that when the length of the data buffer is longer, the amount of added data will be smaller.

Observation 7: The power allocation scheme complies with the traditional *water-filling* mechanism [13]. The allocated power consists of two terms. The first term is associated with the corresponding status of the data buffer and energy queue; the second term depends on the channel gain and transmission distance. From (32) and (33), if the data buffer backlog $\mathbf{Q}_i(t)$ or the backlog difference $\mathbf{Q}_i(t)-\mathbf{Q}_j(t)$ is larger, the first term is larger. This indicates that if the data buffer backlog is larger, it will result in larger allocated power. If the energy queue $\phi_i-\mathbf{E}_i(t)$ is smaller, the first term is also larger. Therefore, if the condition of the battery is better, it can allocate more power. For the second term, the power is a *water-filling* manner over channel fading state.

5.3. Performance Analysis

In this sub-section, we will show that NO-BBA is capable of keeping the data buffer and energy queue stable and guaranteeing the long-term average constraints of the data buffer and battery. Meanwhile, the analytic performance of NO-BBA is presented.

Theorem 4. *For any $V>0$, there exist the constants of $B\geq 0,\epsilon\geq 0,\Psi(\epsilon)$, where $\Psi(\epsilon)$ is less than the optimal network utility $\sum_{k\in\mathcal{K}}U(X_k^{*})$, such that NO-BBA will exhibit the following properties:*

(1) The data buffer $\mathbf{Q}_k(t)$ *and energy queue* $\phi_k - \mathbf{E}_k(t)$ *for sensor node* $k \in \mathcal{K}$ *are mean rate stable. Thus the stable constraint of the data buffer and sustainable constraint of the battery on individual sensor node can be guaranteed;*

(2) The network utility and the average buffer length are bounded by

$$\sum_k U(X_k^*) - \frac{\mathrm{B}}{V} \leq \lim_{N\to\infty} \sup \sum_k U\big\{\tfrac{1}{N}\sum_{t=1}^{N} \mathbb{E}[x_k(t)]\big\} \leq \sum_k U(X_k^*), \quad (38)$$

$$\lim_{N\to\infty} \sup \tfrac{1}{N}\sum_{t=1}^{N}\sum_{k\in\mathcal{K}} \mathbb{E}\{\mathbf{Q}_k(t)\} \leq \frac{\mathrm{B}+[\sum_{\mathrm{k}\in\mathcal{K}} \mathrm{U}(\mathrm{X}_\mathrm{k}^*)-\Psi(\epsilon)]\mathrm{V}}{\epsilon}. \quad (39)$$

Proof: See the appendix Appendix A.

Theorem 4 confirms us that, for any $V > 0$, NO-BBA guarantees the data buffers and energy queues mean stable. The average total data buffer length increases linearly with V, while the achieved network utility is arbitrarily close to the optimal as V increases. This implies a tradeoff of $[O(V), O(\frac{1}{V})]$ between the average buffer length and the gap to the optimal network utility performance.

5.4. Implementation Issues and Special Cases

The previous sub-sections focus on the theoretical analysis of mobile data gathering and energy harvesting in RWSNs, in which both the perfect channel/buffer/ energy state information and centralized scheduling algorithm are explored. In this sub-section, we will discuss some implementation issues, such as computation complexity, the case of lacking channel state information (CSI), and distributed implementation with local buffer and energy status information.

Computation Complexity: The rate control scheme is the minimum of two values, and the close-form expressions of the power allocation scheme are presented in (32), (33) and (36). Thus, the computation complexity of NO-BBA algorithm mainly depends on the computation complexity of the relay selection problem and time slot scheduling problem. The relay selection problem is to select the "best" link among the links from the farther sensor node to all its relay nodes and the sink. This can be solved by choosing the maximum value from a $K+1$-dimension vector, and the number of sensor nodes is less than K. Thus, the worst computation complexity of the relay selection scheme is $O(K^2)$. The time scheduling scheme is to allocate the time slots to the "best"

link of all sensor nodes. Similarly, the worst computation complexity of the time scheduling scheme is $O(K)$. Above all, we can see that the computation complexity is not a critical issue.

Lack of channel state information: In the previous sub-section, the perfect channel state information is utilized to analysis the performance of RWSN. Similar with the works in [23, 30, 38], it is assumed that the performance in wireless channel transmission only depends on the transmission distance. This is a special case of our problem by letting $|h_{ij}(t)|^2 = 1, (\forall i, j)$, and the scheduling scheme would be similar. This case reduces the communication signaling overhead. Meanwhile, it also suffers performance degradation. The impact on performance will be demonstrated by our simulation results to be presented in Section 6.

With only local buffer and energy status: Each sensor node may only have its own buffer and energy status information instead of the global buffer and energy status to design the distributed scheduling algorithm. In this case, the adaptive relay selection could be not employed, and instead the fixed relay selection (namely routing) is applied. For instance, the farther sensor node chooses a near sensor node as its relay only based on the transmission distance. Since the nearer sensor node always harvests more energy, it could take more transmission load, and thus the farther sensor node may choose the sensor node with the nearest distance to the path among its transmission area. Based on the fixed relay selection, the distributed scheduling scheme can be designed as following steps:

1. Rate control similar with that in NO-BBA scheduling scheme;

2. Power control for each sensor node: The transmission power is only dependent on its transmission distance, local buffer and energy status, and it can be derived as $P_{ij}^*(t) = \min\left\{\left[\frac{\mathbf{Q}_i(t)}{\ln 2\mu_i\left[\phi_i - \mathbf{E}_i(t)\right]} - (d_{ij}/d_0)^\alpha L_0(d_0)N_0\right]^\dagger, \frac{\mathbf{E}_i(t)}{T}\right\}$, where j denotes the sink and relay sensor node for the near and far sensor node respectively. Thus the scheduling reward is computed by the weighted transmission rate minus the weighted energy consumption as

$$A_i = \mathbf{Q}_i(t)TW \log_2\left(1 + \frac{P_{ij}^*(t)|h_{ij}(t)|^2}{(d_{ij}(t)/d_0)^\alpha L_0(d_0)N_0}\right) - \mu_i\left[\phi_i - \mathbf{E}_i(t)\right]P_{ij}^*(t)T.$$

3. Distributed time slot contention based on the scheduling reward of each sensor node. One possible approach is to use the method of distributed timers proposed in [3]: upon receiving CTS transmitted by the mobile sink, each sensor node starts a timer whose duration is inversely proportional to its scheduling reward. The timer of the "best" sensor node first expires and a flag packet with duration will be generated to notify the rest of the network about its availability to the time slot.

6. Performance Evaluation

In this section, we report the experimental results obtained from the simulation studies of an RWSN with a mobile sink to show the feasibility and performance of Opt-JoDGE and NO-BBA. Since there are no similar techniques proposed for solving the JoDGE problem, the main parameters are decided according to the typical RWSN settings as well as the parameter values used in related studies. In the experiments, we first evaluated the performance of RF energy harvesting. Then, we studied the performance of Opt-JoDGE and NO-BBA in terms of throughput and network utility. Thirdly, we investigated the efficiency of the *far-relay approach* by comparing it with the direct transmission approach (called one-hop approach). Lastly, the network density issue was investigated and the performance with different number of sensors is presented.

6.1. Simulation Settings

We consider an RWSN with a mobile sink, where 100 sensor nodes are randomly deployed in a $100m \times 50m$ area, and the mobile sink moves along a line ($y_0 = 25, x_0 \in [0, 100]$) with a given speed $v = 1m/s$ to collect data from the sensor nodes. The duration of each time slot T equals $10ms$. Therefore, the total number of time slots in one pass is $N = \frac{100}{vT} = 10000$.

The mobile sink transfers energy to all sensor nodes which use the harvested energy to sense/transmit/receive data. The effective charging distance is 30

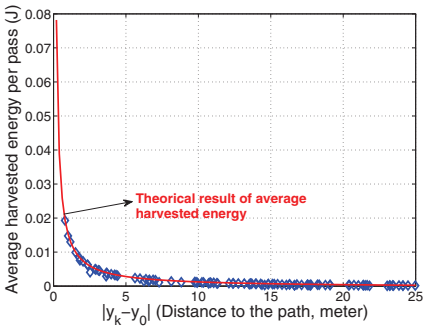

Figure 2: Distance v.s. Average harvested energy per pass.

meters, *i.e.*, $d_e = 30m$. The transmission radius d_k^{tr} of sensor node $k \in \mathcal{K}$ is set to $20m$, which is a parameter that can be adjusted and defined by the power of the transmitter. The distance threshold d_h is $15m$. The average data generation rate $\overline{a}_k$ of sensor node k is set to be $1.5kbps$. The reference path loss is set to be $L_0(d_0) = 100$ with reference distance $d_0 = 1$ meter, and the path loss exponent α is assumed to be 2. Meanwhile, the bandwidth is 20kHz, the average channel gain of small scale fading is 0dB, and the noise power is $N_0 = -60$dBm.

The energy consumed for sensing operation in one time slot is assumed to be 10^{-8} Joule, i.e, $3.6mWh$. As is presented in [20], the energy conversion efficiency ranges from 0.004 to 0.5. In our experiments, we set it to 0.5 for theoretical analysis. Due to the low energy conversion efficiency, how to ensure the harvested energy at each node is always greater than the consumed energy is a critical issue, and we assume that the size of battery is always large enough for storing the harvested energy. Note that as obtained from our experiments, the instantaneous battery is always less than 1 Joule, and the closer sensor nodes have higher energy status due to more harvested energy. For instance, the battery status of the farthest sensor node from the path ranges from $1 * 10^{-4}$ joule to $1.7 * 10^{-4}$ joule, while that of the sensor node closest to the path ranges from 0.90 joule to 0.93 joule. Unless otherwise stated, all simulation runs for at least two hundred passes to obtain statiscally stable results.

6.2. Performance of Energy Harvesting in RWSN with Mobile Sink

In this sub-section, we evaluate the average amount of energy harvested by each sensor node in one pass. We first derive the theoretical performance of energy harvesting, and then compare it with the simulated results.

Given energy transfer radius d_e, only if the sink moves into the region between $(x_k - \sqrt{d_e^2 - (y_k - y_0)^2}, y_0)$ and $(x_k + \sqrt{d_e^2 - (y_k - y_0)^2}, y_0)$, sensor node k is in the energy transfer region and charges its battery. When the sink moves to (x, y_0), the average amount of harvested energy is $\frac{\eta P_s \mathbb{E}[|g_{ks}(i)|^2]}{L_0(d_0)[d_{ks}(x)/d_0]^\alpha}\frac{\Delta x}{v}$, where $\frac{\eta P_s \mathbb{E}[|g_{ks}(i)|^2]}{L_0(d_0)[d_{ks}(x_0)/d_0]^\alpha}$ represents the statistical received power, and $\frac{\Delta x}{v}$ represents the time duration. Thus, the harvested energy is expressed as

$$\begin{aligned}\bar{E}_k &= \int_{x_k-\sqrt{d_e^2-(y_k-y_0)^2}}^{x_k+\sqrt{d_e^2-(y_k-y_0)^2}} \frac{\eta P_s \mathbb{E}[|g_{ks}(i)|^2]}{L_0(d_0)[d_{ks}(x)/d_0]^\alpha}\frac{dx}{v} \\ &= \frac{2\eta P_s \mathbb{E}[|g_{ks}(i)|^2]}{L_0(d_0)|y_k - y_0|}\arctan\Big(\frac{\sqrt{d_e^2-(y_k-y_0)^2}}{|y_k-y_0|}\Big).\end{aligned} \tag{40}$$

Fig. 2 validates the harvested energy derived from the theoretical analysis is consistent with the simulation results. Due to the incomplete symmetric characteristics of the sensor nodes which are close to the start and end point of the pre-defined path, the amount of energy harvested is slightly less than the theoretical results. From Fig. 2, the harvested energy is inversely proportional to the square of distance, *i.e.,* when $|y_k - y_0| \approx 1$, the average harvested energy in one pass is around 0.15 Joule; when $|y_k - y_0| \approx 25$, that is close to 0.0023 Joule. Thus the harvested energy of the sensor nodes closer to the path is much larger than that of the sensor nodes farther away from the path. This observation motivates us to incorporate the *far-relay approach* into the scheduling algorithm.

6.3. Performance Comparison between Opt-JoDGE and NO-BBA

We then present the performance comparison of Opt-JoDGE, NO-BBA, NO-BBA with lacking channel state information and distributed NO-BBA with local buffer and energy status. Since Opt-JoDGE is proved to be optimal, it is used in the experiments as a reference. For NO-BBA, there are three important parameters: V, ϕ_k and $\mu_k (\forall k \in \mathcal{K})$. The parameter V quantifies the tradeoff

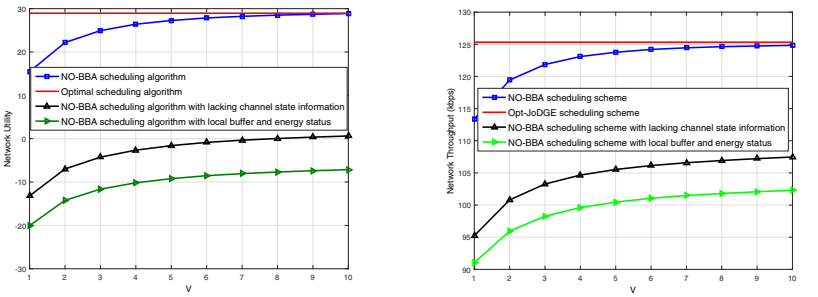

(a) Network Utility Performance (b) Network Throughput Performance

Figure 3: Network utility and network throughput with different V

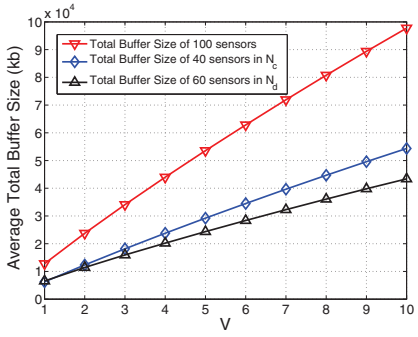

Figure 4: Average total data buffer of sensor nodes with different V.

between the queue backlog and achieved performance. In the simulation, we varied V from 1 to 10 with a step of 1. ϕ_k is constant and set as 1, which can be considered as the battery capacity. The rule of choosing μ_k is to ensure that the first and second terms of lyapunov function $\mathbf{\Theta}(t)$ are in the same order of magnitude. Therefore, we set $\mu_k = \frac{1000V}{5*(\log 2)^2*\phi_k*\overline{a}_k}$.

Fig. 3 presents the performance of network utility and network throughput. The network utility could guarantee the fairness between the transmission rate of each sensor node. While the network throughput only evaluates the sum of average transmission rate of all sensor nodes, the corresponding network throughput maximization (NTM) problem can be formulated by replacing the utility function with $U(X) = X$ and solved with similar method. As shown in

Fig. 3(a), with an increase in V, the network utility of NO-BBA keeps improving and gets closer to the performance of Opt-JoDGE, which is consistent with the analysis in *Theorem* 4. For the performance of network throughput, similar results are obtained such that a larger V results in a higher network throughput. Compared with Opt-JoDGE and NO-BBA, the NO-BBA scheduling scheme with lacking channel state information suffers a throughput and utility loss, and the distributed NO-BBA scheduling scheme with local buffer and energy status suffers a larger utility and throughput loss.

Based on the analysis in *Theorem* 4, the average buffer length of all sensor nodes in NO-BBA is normally proportional to V. A larger V indicates a larger average total data buffer length, which always means larger transmission delay. In Fig. 4, we show the average total data buffer length of all sensor nodes in NO-BBA. We can observe from the figure that a larger V results in a larger data buffer size and the actual total data buffer size increases linearly with V, which is consistent with the analysis. Furthermore, the total data buffer length of the sensor nodes in $\mathcal{N}_c$ and $\mathcal{N}_d$ are also presented in Fig. 4. From the results, we can observe that, even though the number of sensor nodes in $\mathcal{N}_c$ is less than that of sensor nodes in $\mathcal{N}_d$, their total buffer length is larger. This is because the sensor nodes in $\mathcal{N}_c$ harvest less energy and have lower transmission rate.

6.4. Far-relay approach Vs. One-hop approach

In Opt-JoDGE and NO-BBA, the transmission links include not only the links from the sensor nodes to their relay nodes, but also the links to the mobile sink. If only the transmission links from the sensor nodes to the sink are considered, the relay selection problem does not exist and our scheduling scheme will be reduced to the one-hop approach. In this sub-section, we compare the performance of Opt-JoDGE and NO-BBA with both *far-relay approach* and one-hop approach. In order to guarantee all sensor nodes can transmit data to the sink, we set the transmission radius of all sensor nodes to be 25 meters.

The network utility and throughput performance of Opt-JoDGE and NO-BBA with the *far-relay approach* and one-hop approach are presented in Fig. 5.

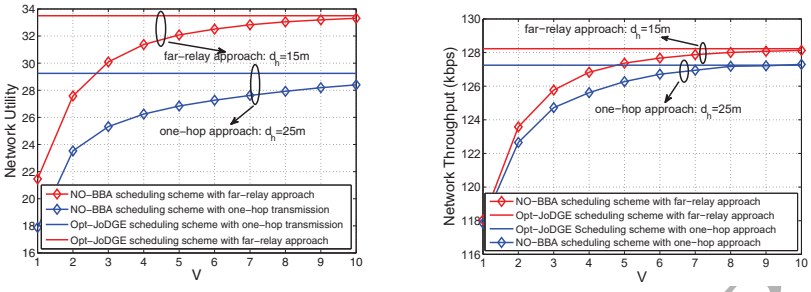

(a) Comparison of Network Utility (b) Comparison of Network Throughput

Figure 5: Performance comparison of network throughput/utility between the far-relay approach and one-hop approach.

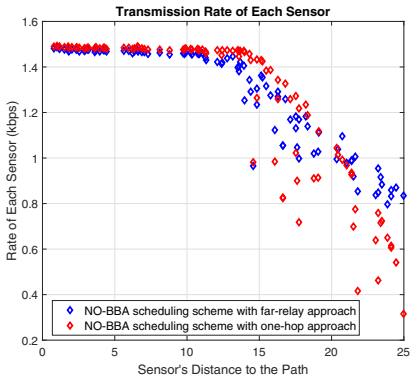

Figure 6: Average transmission rate of each sensor node.

We can observe that the performance of both Opt-JoDGE and NO-BBA with the far-relay approach in terms of both network utility and network throughput is much better than that with the one-hop approach. Furthermore, the network utility improvement is much better than that of network throughput. This is because the *far-relay approach* can improve the performance of the sensor nodes in $\mathcal{N}_c$ and reduce the performance difference between the sensor nodes in $\mathcal{N}_c$ and in $\mathcal{N}_d$, and thus the fairness is improved and the network utility is increased.

Fig. 6 compares the transmission rates of each sensor node in NO-BBA with the *far-relay approach* and one-hop approach. We can observe from Fig.

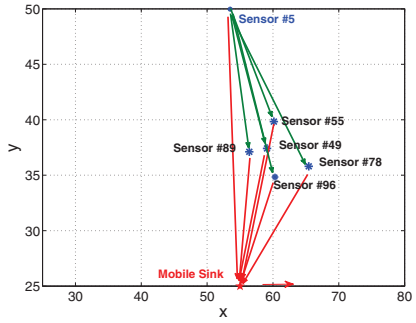

Figure 7: The link connectivity of one example sensor node #5.

Table 2: Number of scheduled time slots for sensor node #5 to its next-hop nodes

Destination	s	#49	#55	#78	#89	#96
# of slots(200 passes)	1498	1856	185	1443	3294	4769
Ratio of slots(%)	11.48	14.28	1.42	11.06	25.25	35.56

6 that the *far-relay* approach can improve the transmission rate of the sensor nodes in $\mathcal{N}_c$. It is because in the *far-relay* approach the sensor nodes in $\mathcal{N}_c$ can select relay sensor nodes in $\mathcal{N}_d$. This decreases both transmission distance and energy consumption. Compared with the one-hop approach, the largest difference amongst the transmission rates of all sensor nodes in the *far-relay approach* is smaller and thus the fairness is improved.

Fig. 7 shows the link connectivity of one example sensor node #5, whose relay node set consists of sensor nodes #49, #55, #78, #89 and #96. In Table 2, we present the number of scheduled time slots for each transmission link starting from sensor node #5. The least number of time slots is allocated to the link between sensor nodes #5 and #55 that has the least harvested energy due to its largest distance to the path. On the other hand, the link between sensor nodes #5 and #96 is scheduled with the largest number of time slots due to the shortest distance. By carefully examining the results in Table 2, we can conclude that the number of scheduled time slots on a transmission link heavily

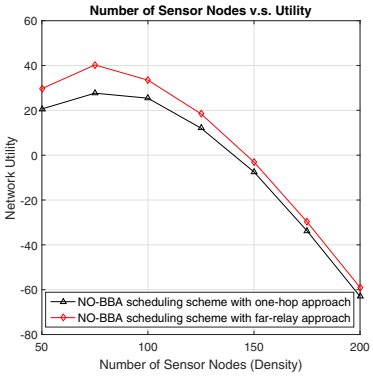

(a) Network utility

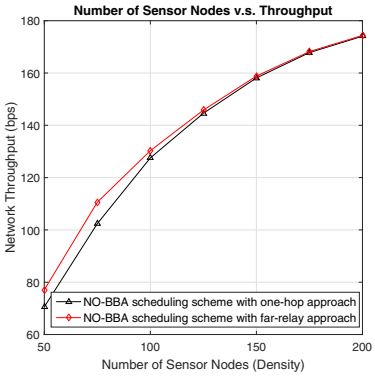

(b) Network throughput

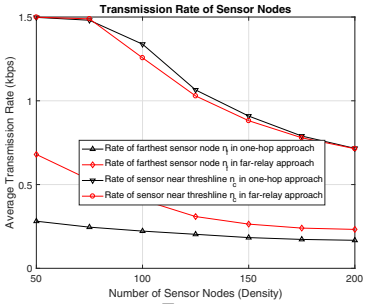

(c) Transmission rates of sensor nodes with different distances

Figure 8: Performance of network utility and throughput with different network densities.

depends on the charging distance from the relay node to the path.

6.5. Performance with different network densities

In this sub-section, we evaluate the performance of network utility and throughput with different network densities, *i.e.*, the number of randomly deployed sensor nodes ranges from 50 to 200. As is shown in Fig. 8(a) and (b), the far-relay approach always performs better than the one-hop approach in terms of both network utility and throughput. Compared with throughput gain, the utility gain introduced by the far-relay approach is larger. It is because both Opt-JoDGE and NO-BBA aim to maximize the network utility instead of

throughput. In Fig. 8(a), one may find that if the number of sensor nodes is increased (e.g., higher density), the network utility first increases and then decreases. It is because the average generated rate $\bar{a}_k$ at a sensor node k is limited to 1.5kbps. Since the network resource is shared by all the sensor nodes, in the case of low density, such as 50 and 75 sensor nodes, the transmission rate of each sensor node is still large, *i.e.*, $\log_2(X) > 0$ if $X > 1$ and $\log_2(X) < 0$ otherwise, and the network utility will increase with more sensor nodes. On the other hand, in a higher network density case, the limited network resource results that the transmission rate of a sensor node is decreasing, even though the number of sensor nodes is larger, the network utility is decreasing.

Fig. 8(c) shows the effects of network density on the transmission rates of the sensor nodes which have different distances from the path. The first one (called n_f) is the farthest sensor node from the path, and the second one (called n_c) is the sensor node that is the closest to the threshold. As shown in Fig. 8(c), the transmission rate of n_f is higher in the far-relay approach compared with the one-hop approach. However, the transmission rate of n_c is slightly lower in the far-relay approach compared with the one-hop approach. This is because in the far-relay approach, the sensor nodes whose distances to the path are the closer to the threshold may act as relays to assist the data transmission of the farther sensor nodes. Furthermore, as shown in Fig. 8(c), with a higher network density, the declined the transmission rate of sensor nodes closer to the threshold is larger than that of the farther sensor nodes. This is because the network fairness is guaranteed in the NUM problem and the rate gap between the two sensor nodes should not be further increased.

7. Conclusion and Future Work

In this paper, we study the joint data gathering and energy harvesting (JoDGE) problem in rechargeable wireless sensor networks (RWSNs) with a mobile sink. Due to the *double near-far* problem introduced by RF energy harvesting, the *far-relay* approach is proposed, in which the sensor nodes closer to

the path may allocate some of the harvested energy to assist the data transmission of other sensor nodes that are farther away. Under the *far-relay* approach, we aim to maximize the network utility by jointly considering the relay selection, power/energy allocation and time scheduling problems. We first derive the optimal joint data gathering and energy harvesting scheduling (Opt-JoDGE) scheme, and then design the near-optimal buffer-battery-aware adaptive scheduling (NO-BBA) algorithm to provide an efficient solution, in which the runtime status of data buffer and battery is considered. The performance of NO-BBA is shown to be close to the optimal scheduling scheme with limited cost of data buffer size. As the future work, we will consider related protocol and algorithm design in RWSNs with mobile sink(s), such as the path planning of one or multiple mobile sinks, relay node placement problem, speed control problem, the optimal number of mobile sinks and so on.

Acknowledgement

This work was supported in part by the National Natural Science Foundation of China (NSFC) under Grant 61771406. We are very grateful to the editors and anonymous reviewers for their valuable guidance, comments and insights to improve the paper.

Appendix A. Proof of Theorem 5.2

For the problem specified in Section 5, there exists a stationary randomized scheme independent of buffer state and energy state, which satisfies

$$\sum_{k\in\mathcal{K}} U\Big\{\frac{1}{N}\sum_{t=1}^{N}\mathbb{E}\big[x_k^*(t)|\mathbf{\Theta}(t)\big]\Big\} = \sum_{k\in\mathcal{K}} U\Big\{\frac{1}{N}\sum_{t=1}^{N}\mathbb{E}\big[x_k^*(t)\big]\Big\} = \Psi(\epsilon), \tag{A.1}$$

$$\frac{1}{N}\sum_{t=1}^{N}\mathbb{E}\Big[x_i^*(t) - \sum_{j\in\mathcal{R}_i\cup s} r_{ij}^*(t)|\mathbf{\Theta}(t)\Big] = \frac{1}{N}\sum_{t=1}^{N}\mathbb{E}\Big[x_i^*(t) - \sum_{j\in\mathcal{R}_i\cup s} r_{ij}^*(t)\Big] \le -\epsilon, \tag{A.2}$$

$$\frac{1}{N}\sum_{t=1}^{N}\mathbb{E}\Big[x_j^*(t) + \sum_{i\in\mathcal{N}_c} r_{ij}^*(t) - r_{js}^*(t)|\mathbf{\Theta}(t)\Big] = \frac{1}{N}\sum_{t=1}^{N}\mathbb{E}\Big[x_j^*(t) + \sum_{i\in\mathcal{N}_c} r_{ij}^*(t) - r_{js}^*(t)\Big] \le -\epsilon, \tag{A.3}$$

$$\frac{1}{N}\sum_{t=1}^{N}\mathbb{E}\Big[\sum_{j\in\mathcal{R}_i\cup s}e^*_{kj}(t)-\widetilde{e}^h_k(t)|\mathbf{\Theta}(i)\Big]=\frac{1}{N}\sum_{t=1}^{N}\mathbb{E}\Big[\sum_{j\in\mathcal{R}_i\cup s}e^*_{kj}(ti)-\widetilde{e}^h_k(t)\Big]=0. \quad \text{(A.4)}$$

Here these expressions can be derived by the similar procedure in [27] and [26].

The design idea behind NO-BBA is to minimize the RHS of (29) over all possible policies. Thus, at each time slot, it yields the following inequality:

$$\begin{aligned}\mathbf{\Delta}\big(\mathbf{\Theta}(t)\big)-V\sum_{k\in\mathcal{K}}U\big\{\mathbb{E}\big[x_k(t)|\mathbf{\Theta}(t)\big]\big\}\le B-V\sum_{k\in\mathcal{K}}U\big\{\mathbb{E}\big[x^*_k(t)|\mathbf{\Theta}(t)\big]\big\}\\+\sum_{i\in\mathcal{N}_c}\Big\{\mathbf{Q}_i(t)\mathbb{E}\Big[x^*_i(t)-\sum_{j\in\mathcal{R}_i\cup s}r^*_{ij}(t)|\mathbf{\Theta}(t)\Big]+\mu_i\big[\phi_i-\mathbf{E}_i(t)\big]\\\mathbb{E}\Big[\sum_{j\in\mathcal{R}_i\cup s}e^*_{ij}-\widetilde{e}^h_i(t)|\mathbf{\Theta}(t)\Big]\Big\}+\sum_{j\in\mathcal{N}_d}\Big\{\mathbf{Q}_j(t)\mathbb{E}\Big[x^*_j(t)+\sum_{i\in\mathcal{N}_c}r^*_{ij}(t)\\+-r^*_{js}(t)|\mathbf{\Theta}(t)\Big]\mu_j\big[\phi_j-\mathbf{E}_j(t)\big]\mathbb{E}\Big[e^{c*}_j-\widetilde{e}^h_j(t)(t)|\mathbf{\Theta}(t)\Big]\Big\}.\end{aligned} \quad \text{(A.5)}$$

Using the sums over the time slot t, adding (A.1), (A.2) , (A.3) and (A.4) into (A.5), and taking expectation, we have

$$\begin{aligned}\frac{1}{N}\sum_{t=1}^{N}\big\{\mathbb{E}\{\mathbf{L}(\mathbf{\Theta}(N+1))\}-\mathbb{E}\{\mathbf{L}(\mathbf{\Theta}(1))\}\big\}-V\frac{1}{N}\sum_{t=1}^{N}\sum_{k\in\mathcal{K}}U\big\{\mathbb{E}[x_k(t)]\big\}\\\le B-V\frac{1}{N}\sum_{t=1}^{N}\sum_{k\in\mathcal{K}}U\big\{\mathbb{E}\big[x^*_k(t)\big]\big\}-\epsilon\frac{1}{N}\sum_{t=1}^{N}\sum_{k\in\mathcal{K}}\mathbb{E}\{\mathbf{Q}_k(t)\}.\end{aligned} \quad \text{(A.6)}$$

(1). Based on Lyapunov function, we can get the following inequality by rearranging (A.6)

$$\mathbb{E}\big\{[\mathbf{Q}_k(t)]^2\big\}\le B*N+\mathbb{E}\{\mathbf{L}(\mathbf{\Theta}(1))\}+V\sum_{t=1}^{N}\sum_{k\in\mathcal{K}}U\big\{\mathbb{E}[x_k(t)]\big\}. \quad \text{(A.7)}$$

Since the utility function is a concave function, we have $\frac{1}{N}\sum_{t=1}^{N}\sum_k U\big\{\mathbb{E}[x_k(t)]\big\}$ $\le\sum_k U\big\{\frac{1}{N}\sum_{t=1}^{N}\mathbb{E}[x_k(t)]\big\}\le\sum_k U(X^*_k)$. And due to the fact that $\big[\mathbb{E}\{|\mathbf{Q}_k(t)|\}\big]^2$ $\le\mathbb{E}\{[\mathbf{Q}_k(t)]^2\}$, we have

$$\mathbb{E}\{|\mathbf{Q}_k(t)|\}\le\sqrt{[B+V\sum_{k\in\mathcal{K}}U(X^*_k)]\cdot N+2\mathbb{E}\big\{\mathbf{L}\big(\mathbf{\Theta}(1)\big)\big\}}. \quad \text{(A.8)}$$

Dividing (A.8) by t and taking a limit as $t\to\infty$ results in $\lim_{t\to\infty}\frac{\mathbb{E}\{|\mathbf{Q}_k(t)|\}}{t}=0$. Hence, the data buffer $\mathbf{Q}_k(t)$ is mean rate stable, and similar proof can be

applied to energy queue $\phi - \mathbf{E}_k(t)$. Thus, the stability constraint of data buffer and feasibility constraint of battery can be guaranteed.

(2). Dividing (A.6) with Vt, rearranging items and using the fact that $\mathbb{E}\{\mathbf{L}(\mathbf{\Theta}(t))\} \geq 0$, we have

$$\frac{1}{N}\sum_{t=1}^{N}\sum_{k\in\mathcal{K}} U\big\{\mathbb{E}[x_k(t)]\big\} \geq \Psi(\epsilon) - \frac{B}{V} - \frac{\mathbb{E}\{\mathbf{L}(\mathbf{\Theta}(1))\}}{VN}. \tag{A.9}$$

Due to the fact that $\frac{1}{N}\sum_{t=1}^{N}\sum_{k\in\mathcal{K}} U\big\{\mathbb{E}[x_k(t)]\big\} \leq \sum_{k\in\mathcal{K}} U\big\{\frac{1}{N}\sum_{t=1}^{N}\mathbb{E}[x_k(t)]\big\}$, we have

$$\sum_{k\in\mathcal{K}} U\big\{\frac{1}{N}\sum_{t=1}^{N}\mathbb{E}[x_k(t)]\big\} \geq \Psi(\epsilon) - \frac{B}{V} - \frac{\mathbb{E}\{\mathbf{L}(\mathbf{\Theta}(1))\}}{VN}. \tag{A.10}$$

Taking a limit as $t \to \infty$ and $\Psi(\epsilon) \to \sum_{k\in\mathcal{K}} U(X_k^*)$ as $\epsilon \to 0$, we can derive the lower bound of network utility. Similarly, we can rewrite (A.6) as

$$\begin{aligned}\frac{1}{N}\sum_{t=0}^{N}\sum_{k\in\mathcal{K}}\mathbb{E}\{\mathbf{Q}_k(t)\} \leq& \frac{B - V\Psi(\epsilon)}{\epsilon} \\ &+ \frac{V}{\epsilon}\sum_{k\in\mathcal{K}}\sum_{k\in\mathcal{K}} U\big\{\frac{1}{N}\sum_{t=1}^{N}\mathbb{E}[x_k(t)]\big\} + \frac{\mathbb{E}\{\mathbf{L}(\mathbf{\Theta}(1))\}}{\epsilon N}.\end{aligned} \tag{A.11}$$

Taking a limit as $t \to \infty$, the upper bound of buffer lenth is derived. Thus the theorem is proved.

References

[1] K. S. Adu-Manu,N. Adam, C. Tapparello, H. Ayatollahi, W. Heinzelman, Energy-harvesting wireless sensor networks (EH-WSNs): A review, ACM Transactions on Sensor Networks (TOSN) 14(2) (2018) 10.

[2] M. H. Anisi, G. Abdul-Salaam, M. Y. I. Idris, A. W. A. Wahab, I. Ahmedy, Energy harvesting and battery power based routing in wireless sensor networks, Wireless Networks 23(1) (2017) 249–266.

[3] A. Bletsas, H. Shin, M. Z. Win, Cooperative communications with outage-optimal opportunistic relaying, IEEE Transactions on Wireless Communications 6(9) (2007) 3450–3460.

[4] S. Boyd, L. Vandenberghe, Convex optimization, Cambridge university press, (2004).

[5] T. Chang, T. Watteyne, K. Pister, Q. Wang, Adaptive synchronization in multi-hop tsch networks, Computer Networks 76 (2015) 165–176.

[6] C. C. Chen, A novel data collection method with recharge plan for rechargeable wireless sensor networks, Wireless Communications and Mobile Computing 2018 (2018).

[7] H. Chen, Y. Li, J. L. Rebelatto, B. F. Uchôa Filho, B. Vucetic], Harvest-then-cooperate: Wireless-powered cooperative communications, IEEE Transactions on Signal Processing 63(7) (2015) 1700–1711.

[8] Cheng, P., He, S., F. Jiang, Y. Gu, J. Chen, Optimal scheduling for quality of monitoring in wireless rechargeable sensor networks, IEEE Transactions on Wireless Communications 12(6) (2013) 3072–3084.

[9] M. Di Francesco, S.K. Das, G. Anastasi, Data collection in wireless sensor networks with mobile elements: A survey, ACM Transactions on Sensor Networks (TOSN) 8(1) (2011) 7.

[10] W. Ejaz, M. Naeem, M. Basharat, A. Anpalagan, S. Kandeepan, Efficient wireless power transfer in software-defined wireless sensor networks, IEEE Sensors Journal 16(20) (2016) 7409–7420.

[11] M. L. Fisher, The lagrangian relaxation method for solving integer programming problems, Management Science 50(12_supplement) (2004) 1861–1871.

[12] S. Gao, H. Zhang, S.K. Das, Efficient data collection in wireless sensor networks with path-constrained mobile sinks, IEEE Transactions on Mobile Computing 10(4) (2011) 592–608.

[13] A. J. Goldsmith, P. P. Varaiya, Capacity of fading channels with channel side information, IEEE Transactions on Information Theory 43(6) (1997) 1986–1992.

[14] S. Guo, F. Wang, Y. Yang, B. Xiao, Energy-efficient cooperative for simultaneous wireless information and power transfer in clustered wireless sensor networks, IEEE Transactions on Communications 63(11) (2015) 4405–4417.

[15] K. Huang, C. Zhong, G. Zhu, Some new research trends in wirelessly powered communications, IEEE Wireless Communications 23(2) (2016) 19–27.

[16] F. P. Kelly, A. K. Maulloo, D. K. Tan, Rate control for communication networks: shadow prices, proportional fairness and stability, Journal of the Operational Research society 49(3) (1998) 237–252.

[17] K. Li, W. Ni, L. Duan, M. Abolhasan, J. Niu, Wireless power transfer and data collection in wireless sensor networks, IEEE Transactions on Vehicular Technology 67(3) (2018) 2686–2697.

[18] R. S. Liu, P. Sinha, C. E. Koksal, Joint energy management and resource allocation in rechargeable sensor networks, In: INFOCOM, 2010 Proceedings IEEE, (2010) 1–9.

[19] W. Lu, Y. Gong, X. Liu, J. Wu, H. Peng, Collaborative energy and information transfer in green wireless sensor networks for smart cities, IEEE Transactions on Industrial Informatics 14(4) (2018) 1585–1593.

[20] X. Lu, P. Wang, D. Niyato, D. I. Kim, Z. Han, Wireless charging technologies: Fundamentals, standards, and network applications, IEEE Communications Surveys & Tutorials 18(2) (2016) 1413–1452.

[21] M. Ma, Y. Yang, Sencar: an energy-efficient data gathering mechanism for large-scale multihop sensor networks, IEEE Transactions on Parallel and Distributed Systems 18(10) (2007).

[22] Z. Mao, C. E. Koksal, N. B. Shroff, Near optimal power and rate control of multi-hop sensor networks with energy replenishment: Basic limitations

with finite energy and data storage, IEEE Transactions on Automatic Control 57(4) (2012) 815–829.

[23] A. Mehrabi, K. Kim, General framework for network throughput maximization in sink-based energy harvesting wireless sensor networks, IEEE Transactions on Mobile Computing 16(7) (2017) 1881–1896.

[24] M. Y. Naderi, K. R. Chowdhury, S. Basagni, Wireless sensor networks with rf energy harvesting: Energy models and analysis, In: Wireless Communications and Networking Conference (WCNC), 2015 IEEE, IEEE (2015) 1494–1499.

[25] P. Nayak, A. Devulapalli, A fuzzy logic-based clustering algorithm for wsn to extend the network lifetime, IEEE sensors journal 16(1) (2016) 137–144.

[26] M. J. Neely, Energy optimal control for time-varying wireless networks. IEEE transactions on Information Theory 52(7) (2006) 2915–2934.

[27] M. J. Neely, Stochastic network optimization with application to communication and queueing systems, Synthesis Lectures on Communication Networks 3(1) (2010) 1–211.

[28] N. T. Nguyen, B. H. Liu, V. T. Pham, C. Y. Huang, Network under limited mobile devices: A new technique for mobile charging scheduling with multiple sinks, IEEE Systems Journal 12(3) (2018) 2186–2196.

[29] P. A. Plonski, P. Tokekar, V. Isler, Energy-efficient path planning for solar-powered mobile robots. Journal of Field Robotics 30(4) (2013) 583–601.

[30] X. Ren, W. Liang, W. Xu, Data collection maximization in renewable sensor networks via time-slot scheduling, IEEE Transactions on Computers 64(7) (2015) 1870–1883.

[31] D. Tse, P. Viswanath, Fundamentals of wireless communication. Cambridge university press, (2005).

[32] T. Wang, Y. Li, G. Wang, J. Cao, M. Z. A. Bhuiyan, W. Jia, Sustainable and efficient data collection from wsns to cloud, IEEE Transactions on Sustainable Computing (2017)

[33] T. Watteyne, J. Weiss, L. Doherty, J. Simon, Industrial ieee802. 15.4 e networks: Performance and trade-offs, In: Communications (ICC), 2015 IEEE International Conference on, IEEE (2015) 604–609.

[34] K. Xie, X. Ning, X. Wang, S. He, Z. Ning, X. Liu, J. Wen, Z. Qin, An efficient privacy-preserving compressive data gathering scheme in wsns, Information Sciences 390 (2017) 82–94.

[35] X. Xu, W. Liang, Monitoring quality optimization in wireless sensor networks with a mobile sink, In: Proceedings of the 14th ACM international conference on Modeling, analysis and simulation of wireless and mobile systems. ACM (2011) 77–84.

[36] H. Yu, Y. Zhang, S. Guo, Y. Yang, L. Ji, Energy efficiency maximization for wsns with simultaneous wireless information and power transfer, Sensors 17(8) (2017) 1906.

[37] J. Zhang, S. J. Liu, P. W. Tsai, F. M. Zou, X. R. Ji, Directional virtual backbone based data aggregation scheme for wireless visual sensor networks, PloS one 13(5) (2018) e0196705.

[38] Y. Zhang, S. He, J. Chen, Near optimal data gathering in rechargeable sensor networks with a mobile sink, IEEE Transactions on Mobile Computing 16(6) (2017) 1718–1729.

[39] M. Zhao, J. Li, Y. Yang, A framework of joint mobile energy replenishment and data gathering in wireless rechargeable sensor networks, IEEE Transactions on Mobile Computing 13(12) (2014) 2689–2705.

[40] P. Zhong, Y. T. Li, W. R. Liu, G. H. Duan, Y. W. Chen, N. Xiong, Joint mobile data collection and wireless energy transfer in wireless rechargeable sensor networks, Sensors 17(8) (2017) 1881.